
























The Identification of Two JWST/NIRCam-Dark Starburst Galaxies at $z = 6.6$ with ALMA

FENGWU SUN ¹, JINYI YANG ², FEIGE WANG ², DANIEL J. EISENSTEIN ¹, ROBERTO DECARLI ³, XIAOHUI FAN ⁴,
GEORGE H. RIEKE ⁴, EDUARDO BAÑADOS ⁵, SARAH E. I. BOSMAN ^{6,5}, ZHENG CAI ⁷, JACLYN B. CHAMPAGNE ⁴,
LUIS COLINA ⁸, FRANCESCO D'EUGENIO ^{9,10}, YOSHINOBU FUDAMOTO ^{11,4}, MINGYU LI ⁷, XIAOJING LIN ^{7,4},
WEIZHE LIU ⁴, JIANWEI LYU ⁴, CHIARA MAZZUCHELLI ¹², XIANGYU JIN ⁴, HYUNSUNG D. JUN ¹³, YUNJING WU ⁷
AND HUANIAN ZHANG ¹⁴

¹Center for Astrophysics | Harvard & Smithsonian, 60 Garden St., Cambridge, MA 02138, USA

²Department of Astronomy, University of Michigan, 1085 S. University Ave., Ann Arbor, MI 48109, USA

³INAF–Osservatorio di Astrofisica e Scienza dello Spazio, via Gobetti 93/3, I-40129, Bologna, Italy

⁴Steward Observatory, University of Arizona, 933 N Cherry Avenue, Tucson, AZ 85721, USA

⁵Max-Planck-Institut für Astronomie, Königstuhl 17, 69117 Heidelberg, Germany

⁶Institute for Theoretical Physics, Heidelberg University, Philosophenweg 12, D–69120, Heidelberg, Germany

⁷Department of Astronomy, Tsinghua University, Beijing 100084, China

⁸Centro de Astrobiología (CAB), CSIC-INTA, Ctra. de Ajalvir km 4, Torrejón de Ardoz, E-28850, Madrid, Spain

⁹Kavli Institute for Cosmology, University of Cambridge, Madingley Road, Cambridge, CB3 0HA, United Kingdom

¹⁰Cavendish Laboratory - Astrophysics Group, University of Cambridge, 19 JJ Thomson Avenue, Cambridge, CB3 0HE, United Kingdom

¹¹Center for Frontier Science, Chiba University, 1-33 Yayoi-cho, Inage-ku, Chiba 263-8522, Japan

¹²Instituto de Estudios Astrofísicos, Facultad de Ingeniería y Ciencias, Universidad Diego Portales, Avenida Ejercito Libertador 441, Santiago, Chile

¹³Department of Physics, Northwestern College, 101 7th St SW, Orange City, IA 51041, USA

¹⁴Department of Astronomy, Huazhong University of Science and Technology, Wuhan, Hubei 430074, China

(Received June 10, 2025)

Submitted to ApJ

ABSTRACT

We analyze two dusty star-forming galaxies at $z = 6.6$. These galaxies are selected from the ASPIRE survey, a JWST Cycle-1 medium and ALMA Cycle-9 large program targeting 25 quasars and their environments at $z \simeq 6.5 - 6.8$. These galaxies are identified as **companions to UV-luminous quasars** and **robustly detected in ALMA continuum and [C II]** emission, yet they are extraordinarily faint at the NIRCam wavelengths (down to > 28.0 AB mag in the F356W band). They are more obscured than galaxies like Arp220, and thus we refer to them as “NIRCam-dark” starburst galaxies (star formation rate $\simeq 80 - 250 M_{\odot} \text{yr}^{-1}$). Such galaxies are typically missed by (sub)-millimeter blank-field surveys. From the star-formation history (SFH), we show that the NIRCam-dark galaxies are viable progenitors of massive quiescent galaxies at $z \gtrsim 4$ and descendants of UV-luminous galaxies at $z > 10$. Although it is hard to constrain their number density from a quasar survey, we conclude that NIRCam-dark galaxies can be as abundant as $n \sim 10^{-5.5} \text{Mpc}^{-3}$ assuming a light halo occupation model. If true, this would equal to $\sim 30\%$ of the number densities of both the quiescent galaxies at $z \gtrsim 4$ and UV-luminous galaxies at $z > 10$. We further predict that analogs at $z \sim 8$ should exist according to the SFH of early massive quiescent galaxies. However, they may fall below the current detection limits of wide JWST and ALMA surveys, thus remaining “JWST-dark”. To fully trace the evolution of massive galaxies and dust-obscured cosmic star formation at $z \gtrsim 8$, wide-field JWST/NIRCam imaging and slitless spectroscopic surveys of early protoclusters are essential.

Keywords: High-redshift galaxies (734) — Starburst galaxies (1570) — Luminous infrared galaxies (946) — Galaxy evolution (594) — James Webb Space Telescope (2291)

1. INTRODUCTION

Dust plays a pivot role in obscuring the majority of the cosmic star formation at redshift $z \simeq 1 - 4$ (see a review by P. Madau & M. Dickinson 2014). Since the end of the last century, dusty star-forming galaxies (DSFGs) with IR lu-

minosities resembling those of local ultra-luminous infrared galaxies (ULIRGs; $L_{\text{IR}} \simeq 10^{12} - 10^{13} L_{\odot}$) have been found in abundance across the bulk of the cosmic history (e.g., I. Smail et al. 1997; D. H. Hughes et al. 1998; J. D. Vieira et al. 2010; S. J. Oliver et al. 2012 and reviews by, e.g., J. A. Hodge & E. da Cunha 2020). These galaxies, also known as submillimeter galaxies (SMGs), undergo vigorous starbursts with star formation rates (SFR) greater than $100 M_{\odot} \text{ yr}^{-1}$, while only emitting a very small fraction of their light in the rest-frame UV/optical because of the strong dust obscuration. When they exhaust their cold molecular gas reservoirs, DSFGs are believed to evolve into massive quiescent galaxies at lower redshifts (e.g., S. Toft et al. 2014).

Among all DSFGs discovered at (sub)-millimeter wavelengths, the optically faint DSFG population has been of particular interest. Simply placing the same DSFG from $z = 0.5$ to higher redshifts, the brightness of the galaxy will drop quickly in the optical–IR, but remain almost unchanged at millimeter wavelengths because of the strong negative K correction. Therefore, a low flux density ratio between the rest-frame optical and far-IR is indicative of a high photometric redshift. Indeed, one of the first DSFGs discovered at $850 \mu\text{m}$, HDF850.1 (D. H. Hughes et al. 1998), remains undetected with HST from the optical to near-IR. The redshift of HDF850.1 is confirmed at $z = 5.18$ through CO and [C II] spectroscopy with millimeter interferometry (F. Walter et al. 2012). After more than two decades since its discovery, the stellar component of HDF850.1 was finally detected at $1\text{--}5 \mu\text{m}$ with JWST/NIRCam (F. Sun et al. 2024; T. Herard-Demanche et al. 2025). Similar galaxies have been referred to as “HST-dark”, “near-IR-dark”, “H-dropout”, or “H-faint” galaxies in a plethora of literature. These galaxies are found to have a wide range of redshift ($z \simeq 2 - 6$), stellar age and dust attenuation distribution, and they consist of 15-20% of DSFGs selected through ALMA millimeter observations (e.g., C.-C. Chen et al. 2015; J. M. Simpson et al. 2015; M. Franco et al. 2018; T. Wang et al. 2019; Y. Yamaguchi et al. 2019; C. Gómez-Guijarro et al. 2022; S. Fujimoto et al. 2024).

So far, the vast majority of DSFGs selected through (sub)-millimeter surveys in blank fields are at $z \lesssim 6$ (e.g., J. M. Simpson et al. 2019; M. Aravena et al. 2020; U. Dudzevičiūtė et al. 2020; C. Gómez-Guijarro et al. 2022; L. Bing et al. 2023; S. Fujimoto et al. 2024; A. S. Long et al. 2024a). At $z \gtrsim 6$, the Epoch of Reionization (EoR), the detections of DSFGs frequently rely on gravitational lensing (e.g., D. A. Riechers et al. 2013; D. Watson et al. 2015; M. L. Strandet et al. 2017; J. A. Zavala et al. 2018; N. Laporte et al. 2021) and pointed ALMA observations of known luminous galaxies and quasars (e.g., R. Decarli et al. 2017; C. Mazzucchelli et al. 2019; B. P. Venemans et al. 2019; T. Hashimoto et al. 2019; Y. Tamura et al. 2019; Y. Harikane et al. 2020; H. Inami et al. 2022; A. P. S. Hygate et al. 2023), especially through the Cycle-7 ALMA large program REBELS (R. J. Bouwens et al. 2022). Many of these pointed observations succeeded in detecting the dust-obscured star formation not only in the targeted galaxies, but also their companions that

could be totally obscured in the HST bands, and sometimes even Spitzer/IRAC $3.6/4.5 \mu\text{m}$ (e.g., Y. Fudamoto et al. 2021; S. Fujimoto et al. 2024).

These studies highlight the importance of dust-obscured star formation even in the EoR, although the measurements of obscured SFR densities based on these pointed (and thus biased) observations remain highly challenging (e.g., see H. S. B. Algera et al. 2023; I. F. van Leeuwen et al. 2024). If heavily obscured galaxies frequently exist at these redshifts but below the detection limit of wide-field imaging surveys, our understanding of massive galaxy assembly would be highly incomplete. In fact, JWST imaging and spectroscopic observations of early massive quiescent galaxies frequently imply the existence of starburst progenitors at $z \simeq 6\text{--}10$ with SFR above $100 M_{\odot} \text{ yr}^{-1}$ (e.g., A. C. Carnall et al. 2023a; K. Glazebrook et al. 2024; A. de Graaff et al. 2025; W. M. Baker et al. 2025). Some of these progenitors may have undergone highly efficient starbursts, converting the majority of accreted baryons to stars (e.g., A. C. Carnall et al. 2024; C. Turner et al. 2025). Associated with the starburst, these galaxies may be heavily dust-obscured and thus remain as an undetected population with JWST wide-field imaging surveys (e.g., C. C. Williams et al. 2024; K. Glazebrook et al. 2024).

In this work, we present the identification and analyses of two NIRCam-dark galaxies at $z = 6.6$ with ALMA. These two dusty starburst galaxies are selected through the ASPIRE JWST and ALMA survey (F. Wang et al. 2023, in prep.). In Section 2, we describe the observations and data processing techniques. We present the source selection, photometry and SED modeling in Section 3. We discuss the implications of these galaxies to the overall picture of massive galaxy evolution in Section 4. Our conclusions are summarized in Section 5. Throughout this work, we assume a flat Λ CDM cosmology with $H_0 = 70 \text{ km s}^{-1} \text{ Mpc}^{-1}$ and $\Omega_M = 0.3$. AB magnitude system (J. B. Oke & J. E. Gunn 1983) is adopted to describe source brightness in the optical and near-IR. We also assume a G. Chabrier (2003) initial mass function. We define the IR luminosity (L_{IR}) as the integrated luminosity over a rest-frame wavelength range from 8 to $1000 \mu\text{m}$.

2. OBSERVATION AND DATA PROCESSING

2.1. JWST/NIRCam

JWST/NIRCam (M. J. Rieke et al. 2023) three-band imaging data of 25 luminous quasars at $z = 6.5 - 6.8$ were obtained through the Cycle-1 ASPIRE program (GO-2078; PI: F. Wang; F. Wang et al. 2023). The exposure time with each filter is 1417 s (F115W), 2834 s (F200W) and 1417 s (F356W), respectively. The NIRCam data processing has been described in detail with previous papers from the ASPIRE collaboration (F. Wang et al. 2023; J. Yang et al. 2023). Briefly, the data were processed through a modified JWST calibration pipeline (H. Bushouse et al. 2023) with the reference file `jwst_1080.pmap` (including JWST Cycle-1 NIRCam flux calibrations). This includes a few commonly adopted customized treatments, for example, $1/f$ noise subtraction, iterative sky background removal and WCS align-

ment to Gaia DR3 (Gaia Collaboration et al. 2023) or the DESI Legacy Imaging Survey (A. Dey et al. 2019) if not enough Gaia stars are found within the Field of View (FoV).

We also note that ASPIRE also obtained NIRCcam wide-field slitless spectroscopy (WFSS) of the targeted quasar fields in the F356W band. These data were not directly used in our analyses (but see Section 4.2).

2.2. ALMA

ALMA 1.2 mm mosaics of all 25 ASPIRE quasar fields were obtained through a 100-hr ALMA Cycle-9 large program (PI: F. Wang; Program ID: 2022.1.01077.L). In each quasar field, we map the $1'.2 \times 1'.1$ region centered on the quasar at the [C II] 158 μm wavelength, and therefore search for companion galaxies at the quasar redshifts (within a velocity offset of $\Delta v \sim \pm 2200 \text{ km s}^{-1}$).

The ALMA data reduction has been described in detail by F. Sun et al. (2025a) through a standard CASA v6.4.1.12 pipeline (CASA Team et al. 2022). To avoid the artificial boost of continuum flux densities from [C II] emitters at quasar redshifts, we first flagged the spectral channels that have a velocity offset smaller than 500 km s^{-1} from the quasar [C II] line center. To optimize the detection of sources with both compact and extended dust continuum or [C II] emissions, we produced ALMA mosaics at both native resolution (Briggs weighting `robust=0.5`, no uv tapering) and tapered resolution (`robust=2.0`, uv tapered with a Gaussian kernel of $\text{FWHM}=1''$). The synthesized beam FWHM is $0''.65 \pm 0''.05$ and $1''.34 \pm 0''.05$ for native and tapered continuum image mosaics, respectively. The typical continuum rms noises (before primary beam response correction) of our ALMA mosaics are $0.031 \pm 0.004 \text{ mJy beam}^{-1}$ and $0.034 \pm 0.004 \text{ mJy beam}^{-1}$ at native and tapered resolution, respectively.

We also include archival ALMA measurements of our targets at Band 3, 4, 5 and 7. Band-3, 4, 5 observations were obtained through program 2017.1.00139.S, 2017.1.01532.S and 2019.1.00147.S (B. P. Venemans et al. 2019; A. Pensabene et al. 2021; J. Li et al. 2022). We directly use these published photometric measurements. Band 7 observations were obtained through 2021.1.00443.S (PI: J. Spilker), and the data were processed through a similar routine as that of the ASPIRE-ALMA data.

3. RESULTS

3.1. The identification of NIRCcam-dark galaxies

F. Sun et al. (2025a) reported the detection of 117 continuum sources at primary beam response ≥ 0.25 (over 35 arcmin^2) through the ASPIRE-ALMA survey. Among these 1.2-mm continuum sources, 23 sources are quasars and the remaining sources are classified as DSFGs at cosmological distances. Six of these DSFGs are at $z > 6$, all confirmed as quasar companions through ALMA [C II] detection or JWST/NIRCcam grism spectroscopy of the [O III] doublets.

Among all ASPIRE-ALMA continuum sources, we identify two galaxies detected at 1.2 mm at high significance

(8.7 and 26.4σ) but lacking obvious NIRCcam counterparts. The NIRCcam and ALMA images of these two galaxies are shown in Figure 1. Both galaxies are spectroscopically confirmed as companions to quasars at $z \sim 6.6$ through ALMA [C II] spectroscopy. The first source, J0305m3150.C05 ($z = 6.606$), was known as a companion galaxy to quasar J0305–3150 at $z = 6.614$ through previous ALMA studies (dubbed as C3; e.g., B. P. Venemans et al. 2019, 2020; J. Li et al. 2022; F. Wang et al. 2023) with a velocity offset of $\Delta v = -290 \pm 30 \text{ km s}^{-1}$ and angular offset of $6''.9$. The second source, J1526m2050.C02 ($z = 6.590$), was also known as a companion galaxy to quasar J1526–2050 (or PSO J231–20, $z = 6.587$) through previous ALMA studies (R. Decarli et al. 2017; C. Mazzucchelli et al. 2019; A. Pensabene et al. 2021) with a velocity offset of $\Delta v = +137 \pm 30 \text{ km s}^{-1}$ and angular offset of $1''.6$. The detections with multiple ALMA datasets at various frequencies validate the fidelity of these sources.

We conduct photometry of the two sources in available JWST/NIRCcam and ALMA data. Because J1526m2050.C02 is close to the luminous quasar, we subtract a point spread function (PSF) model from the quasar image. The PSF model is constructed using a PSF star library in the ASPIRE fields. The detailed method and validation of the PSF model and subtraction will be presented in a forthcoming paper from the ASPIRE collaboration (J. Yang et al. in prep.). The quasar-subtracted NIRCcam images in the F200W and F356W bands are shown in the third row of Figure 1.

Compared with the ALMA continuum contours, we find faint diffuse emission (diameter $\sim 1''$) at the location of J1526m2050.C02 in the F356W band. This is somewhat expected, because the surface brightness dimming is as a function of $(1+z)^{-4}$, and DSFGs at lower redshifts are known to host more extended stellar continuum (attenuated) than the dust continuum (e.g., C.-C. Chen et al. 2015; J. A. Hodge et al. 2016). Therefore, to avoid substantial flux loss of diffuse emission, we obtain photometry using a circular aperture of radius $r = 0''.5$. The photometric uncertainties are estimated using random apertures in source-free regions within $10''$ from the targets. We find that J0305m3150.C05 remains undetected in all NIRCcam images ($> 28.0 \text{ AB mag}$ in F356W, 3σ limit), and the residuals of J1526m2050.C02 are only detected in the F356W band ($26.5 \pm 0.1 \text{ AB mag}$).

These two DSFGs are extraordinarily faint at the NIRCcam wavelengths. For comparison, all 289 DSFGs in J. McKinney et al. (2025) that fall in COSMOS-Web footprint (C. M. Casey et al. 2023) are brighter than 26 AB mag in the F444W band if measured with the same $r = 0''.5$ aperture size. To our knowledge, DSFGs similar to J0305m3150.C05 or J1526m2050.C02 do not exist in ALMA blank-field surveys in the Hubble Ultra-Deep Field (HUDF) / GOODS-S region either (e.g., J. S. Dunlop et al. 2017; B. Hatsukade et al. 2018; M. Franco et al. 2018; J. González-López et al. 2020; C. Gómez-Guijarro et al. 2022), as all secure ($> 6\sigma$) ALMA continuum sources have been detected by NIRCcam (e.g., L. A. Boogaard et al. 2024; R. Hill et al. 2024) as long as they fall in the JADES footprints (D. J. Eisenstein et al. 2023). Therefore, we refer to these galaxies as “NIRCcam-

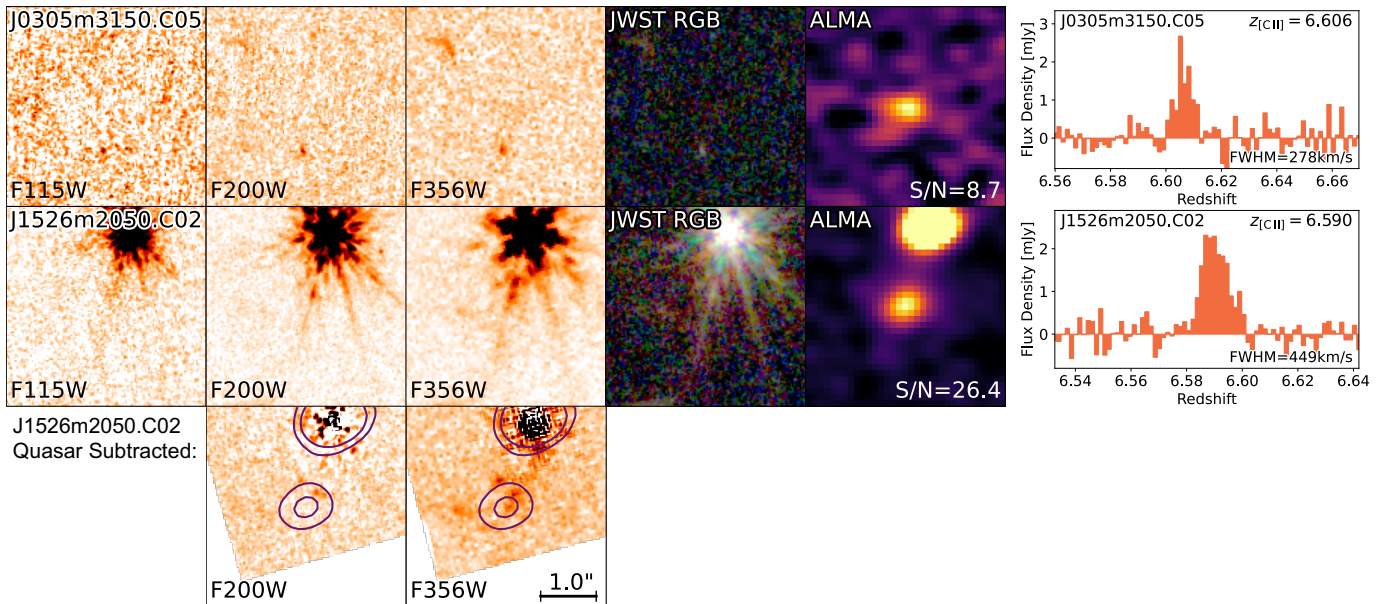


Figure 1. JWST NIRCам images (F115W, F200W, F356W), ALMA 1.2 mm continuum images and [C II] 158 μm spectra of two NIRCам-dark galaxies at $z_{\text{spec}} \sim 6.6$. Because the luminous quasar J1526–2050 is visible to the northwest of J1526m2050.C02 ($1''.6$ separation), we also show the quasar-subtracted F200W and F356W image of J1526m2050.C02 in the third row, with ALMA continuum contours (purple) at 10 and 20σ overlaid. Image size is $4'' \times 4''$. These galaxies are selected as companions of quasars with ALMA, but remain undetected or faint at JWST/NIRCам wavelengths.

dark” ($S_{3.6\mu\text{m}}/S_{1.2\text{mm}} < 10^{-4}$) starburst galaxies in this paper.

ALMA Band-6/7 flux densities are measured from the peak of the uv -tapered images as described by F. Sun et al. (2025a). ALMA flux densities in other bands are taken from literature (A. Pensabene et al. 2021; J. Li et al. 2022). We also measure the ALMA 1.17 mm continuum sizes using CASA IMFIT function in the image plane with synthesized beam deconvolved. Both sources have compact dust continuum emission with circularized effective radius $R_{e,\text{circ}} \sim 0''.19$ (~ 1 kpc at $z = 6.6$). Table 1 summarizes the JWST and ALMA photometry of the two NIRCам-dark DSFGs.

3.2. SED modeling and physical properties

We model the spectral energy distributions (SED) of the two NIRCам-dark galaxies with CIGALE, an energy-balance parametric SED-fitting software (S. Noll et al. 2009; M. Boquien et al. 2019). We assume a commonly used delayed- τ star-formation history (SFH), in which $\text{SFR}(t) \propto t \exp(-t/\tau)$ and τ is the peak time of star formation. We allow the age of main stellar population to be 20–500 Myr and τ to be 20–2000 Myr. An optional late starburst is allowed in the last 20 Myr of SFH, which could produce up to 10% of the total stellar mass. We use G. Bruzual & S. Charlot (2003) stellar population synthesis models, and assume a solar metallicity (Z_{\odot}) given the strong presence of dust. We adopt a modified D. Calzetti et al. (2000) attenuation curve, and allow the variation of the power-law slope by ± 0.2 and A_V effectively at 0–15. Nebular emission is included assuming an electron density of $n_e = 100 \text{ cm}^{-3}$ and ionization parameter $\log U = -4 \sim -2$. For simplic-

Table 1. The properties of the two NIRCам-dark galaxies.

| | J0305m3150.C05 | J1526m2050.C02 |
|--|-----------------|-----------------|
| R.A [deg] | 46.31826 | 231.65781 |
| Decl. [deg] | −31.84859 | −20.83397 |
| z_{spec} | 6.606 | 6.590 |
| Offset from quasar ["] | 6.9 | 1.6 |
| $R_{e,\text{circ}}$ ["] | 0.19 ± 0.08 | 0.19 ± 0.05 |
| NIRCам F115W [nJy] | <56.4 | <81.6 |
| NIRCам F200W [nJy] | <24.6 | <40.8 |
| NIRCам F356W [nJy] | 11.6 ± 7.7 | 87.8 ± 8.7 |
| ALMA 0.893 mm [mJy] | 0.64 ± 0.04 | 1.71 ± 0.04 |
| ALMA 1.17 mm [mJy] | 0.32 ± 0.04 | 1.04 ± 0.04 |
| $\log[M_{\text{star}}/M_{\odot}]$ | 10.0 ± 0.5 | 10.5 ± 0.5 |
| $\log[\text{SFR}/M_{\odot} \text{ yr}^{-1}]$ | 1.9 ± 0.1 | 2.4 ± 0.1 |
| A_V [mag] | 7.5 ± 3.7 | 3.5 ± 0.4 |
| $\log[L_{\text{IR}}/L_{\odot}]$ | 11.9 ± 0.1 | 12.4 ± 0.1 |
| $\log[M_{\text{gas}}/M_{\odot}]$ | 9.5 ± 0.2 | 10.4 ± 0.2 |
| $\log[M_{\text{dust}}/M_{\odot}]$ | 7.6 ± 0.3 | 8.3 ± 0.1 |
| T_{dust} [K] | 44.7 ± 10.9 | 36.5 ± 2.4 |

NOTE—The circularized effective radii ($R_{e,\text{circ}}$) are measured at ALMA 1.17 mm (dust continuum). The molecular gas masses (M_{gas}) are from J. Li et al. (2022, J0305m3150.C05) and A. Pensabene et al. (2021, J1526m2050.C02). Other ALMA photometry is also available therein. Upper limits are at 3σ .

ity, we assume a mid-to-far-IR dust continuum model from C. M. Casey (2012), parameterized by the dust temperature (T_{dust} ; 30–60 K), dust emissivity (β_{em} ; 1.6–2.0) and mid-IR power-law slope (α_{MIR} , fixed at 2.0). Although the C. M. Casey (2012) model does not include mid-IR polycyclic aro-

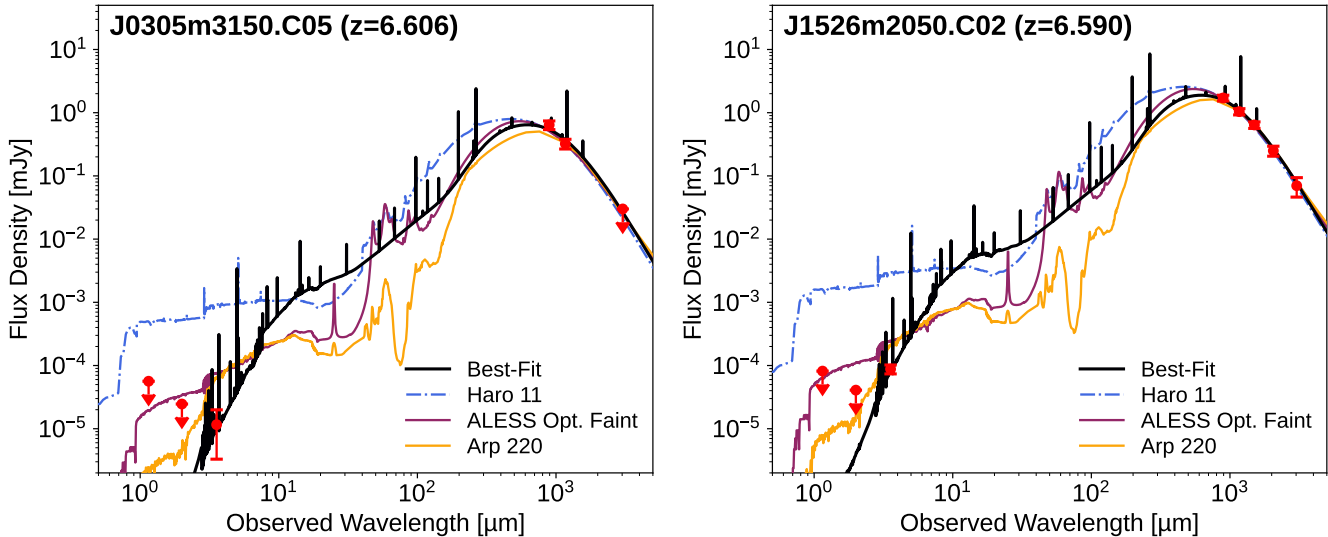


Figure 2. SEDs of the two NIRCcam-dark galaxies (red circles). The best-fit SED models obtained by CIGALE are shown in the black lines. The SED templates of Haro 11 (nearby starburst galaxy, blue; J. Lyu et al. 2016), Arp 220 (nearby ULIRG, orange; L. Silva et al. 1998) and ALESS optically faint DSFGs at $z \sim 3$ (purple; E. da Cunha et al. 2015), all redshifted and scaled to the ALMA 1.2-mm flux densities, are shown for comparison.

matic hydrocarbon (PAH) features, the inclusion of a mid-IR power-law slope can well reproduce the luminosity excess from PAHs from a comparison of widely used empirical SED templates (e.g., R. Chary & D. Elbaz 2001; G. H. Rieke et al. 2009) as tested by F. Sun et al. (2025a).

We note that an active galactic nucleus (AGN) component is not included in our SED modeling. Both sources remain undetected in the X-ray with Chandra (T. Connor et al. 2020; F. Wang et al. 2021), disfavoring the presence of unobscured AGNs. The AGN contributions to the ALMA flux densities are also likely insignificant (see the discussion in F. Sun et al. 2025a).

Figure 2 shows the best-fit SED models of the two NIRCcam-dark galaxies. For comparison, we also plot the SED templates of (i) the nearby starburst galaxy Haro 11 (J. Lyu et al. 2016, whose far-IR SED may resemble those of luminous DSFGs at $z \gtrsim 6$ as argued by M. E. De Rossi et al. 2018), (ii) the nearby ULIRG Arp 220 (L. Silva et al. 1998, including both the obscured nucleus and unobscured stellar component) and (iii) the optically faint DSFGs at $z \sim 3$ selected through the ALESS survey (E. da Cunha et al. 2015), all normalized to the ALMA 1.2-mm flux densities. We find that the two NIRCcam-dark galaxies appear to be more obscured in rest-frame optical even compared with Arp 220 or $z \sim 3$ optically faint DSFGs. In particular, $z \sim 3$ optically faint DSFGs in E. da Cunha et al. (2015) will remain above our F200W and F356W detection limit if they are redshifted to $z = 6.6$. The SED fitting implies a substantial V -band dust attenuation (A_V up to 7.5 ± 3.7 mag for J0305m3150.C05) for these NIRCcam-dark DSFGs.

The multiple-wavelength ALMA observations offer useful constraints to the far-IR SEDs. With IR luminosities $L_{\text{IR}} \simeq 10^{11.9} - 10^{12.4} L_{\odot}$, we infer a dust-obscured SFR

of $80\text{--}250 M_{\odot} \text{ yr}^{-1}$ for the two sources (R. C. Kennicutt & N. J. Evans 2012). These are consistent with the SFR inferred from the [C II] luminosities (A. Pensabene et al. 2021; J. Li et al. 2022). In contrast, the constraints on their stellar mass are rather poor. We infer stellar mass $\log(M_{\text{star}}/M_{\odot})$ of 10.0 ± 0.5 and 10.5 ± 0.5 for both targets respectively, and the large errors are natural consequence of poor constraints in the rest-frame UV/optical through Bayesian inference. The inferred physical properties of the two galaxies are also presented in Table 1.

The molecular gas masses (M_{gas}) of the two galaxies have been studied through [C I] and CO observations by A. Pensabene et al. (2021) and J. Li et al. (2022). We find comparable M_{gas} and M_{star} for the two galaxies, indicating high gas fractions associated with the starbursts. We further model the far-IR SEDs of the two galaxies with a modified blackbody model assuming a dust absorption coefficient as $\kappa = 0.40 \times (\nu/250)^{\beta_{\text{em}}}$ in unit of $\text{cm}^2 \text{ g}^{-1}$, where ν is the rest-frame frequency in GHz and β_{em} is fixed at 1.8 following previous works (e.g., T. Díaz-Santos et al. 2017; F. Sun et al. 2022). We also consider the CMB heating effect following E. da Cunha et al. (2013), which is found to be small at the derived T_{dust} . The derived dust masses and temperatures are also presented in Table 1. Although the constraints are poor for J0305m3150.C05 because of limited ALMA coverage, both sources exhibit normal dust temperature and gas-to-dust ratio δ_{GDR} around 100.

4. DISCUSSION

4.1. Placing NIRCcam-dark starbursts in the context of massive galaxy evolution

These two NIRCcam-dark galaxies are among the highest-redshift ALMA continuum sources selected by the ASPIRE-

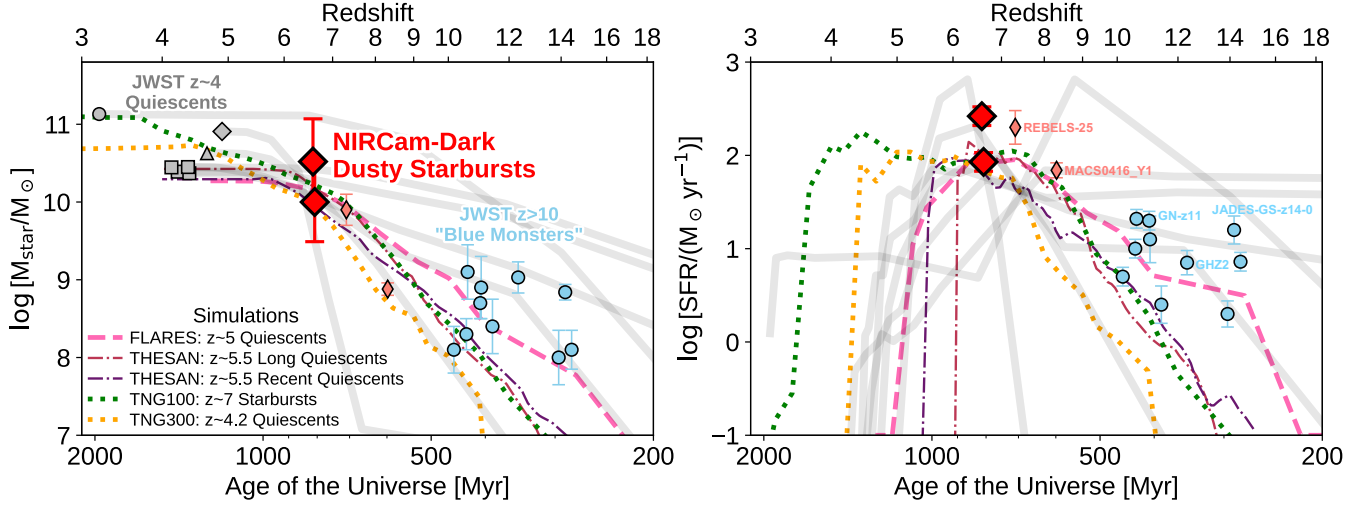


Figure 3. Stellar mass (left) and SFR (right) versus redshift for NIRCam-dark dusty starburst galaxies (red diamonds) in the context of massive galaxy evolution. For comparison we show the star-formation histories of massive quiescent galaxies at $z \sim 4$ confirmed with JWST spectroscopy (gray circle: K. Glazebrook et al. 2024 but using the SFH from C. Turner et al. 2025; diamond: A. de Graaff et al. 2025 with solar-metallicity SFH model; triangle: A. C. Carnall et al. 2023a but using the SFH from Z. Ji et al. 2024a; squares: W. M. Baker et al. 2025). We also highlighted two ALMA-confirmed dusty starbursts known at $z > 7$ prior to JWST in coral diamonds, including REBELS-25 ($z = 7.3$; A. P. S. Hygate et al. 2023) and MACS0416_Y1 ($z = 8.3$; Y. Tamura et al. 2019). JWST-confirmed luminous galaxies at $z > 10$ with low dust content (also known as “blue monsters”; e.g., F. Ziparo et al. 2023) are shown in blue circles (including P. Arrabal Haro et al. 2023; A. J. Bunker et al. 2023; S. Carniani et al. 2024; M. Castellano et al. 2024; T. Y.-Y. Hsiao et al. 2024; V. Kokorev et al. 2025; R. P. Naidu et al. 2025; J. A. Zavala et al. 2025). The median evolution track of early massive galaxies in cosmological simulations are shown in colored lines (including FLARES, C. C. Lovell et al. 2023; IllustrisTNG, A. Pillepich et al. 2018, D. Nelson et al. 2019 and A. I. Hartley et al. 2023; THESAN, R. Kannan et al. 2022 and H. G. Chittenden et al. 2025). NIRCam-dark dusty starburst galaxies presented by this study are candidates for the progenitors of massive quiescent galaxies at $z \sim 4$ and descendants of “blue monsters” at $z > 10$.

ALMA survey. The redshifts of our targets are also higher than the vast majority of DSFGs selected from millimeter surveys in blank fields ($z \lesssim 6$; see references in Section 1). Therefore, a low flux density ratio of $S_{3.6\mu\text{m}}/S_{1.2\text{mm}}$ is somewhat expected at such high redshifts (e.g., Y. Yamaguchi et al. 2019), leading to the faintness of these galaxies at NIRCcam wavelengths.

However, from the viewpoint of massive galaxy evolution, the identification of NIRCcam-dark galaxies in the EoR could be particularly important. Figure 3 shows the stellar mass and SFR of NIRCcam-dark galaxies compared with (i) the SFH of massive quiescent galaxies at $z \gtrsim 4$ that have been frequently confirmed with JWST spectroscopy (e.g., A. C. Carnall et al. 2023a; K. Glazebrook et al. 2024; W. M. Baker et al. 2025; A. de Graaff et al. 2025), and (ii) $z > 10$ luminous galaxies with low dust content confirmed by JWST (e.g., P. Arrabal Haro et al. 2023; A. J. Bunker et al. 2023; S. Carniani et al. 2024; M. Castellano et al. 2024; V. Kokorev et al. 2025; R. P. Naidu et al. 2025; J. A. Zavala et al. 2025; also known as “blue monsters”, e.g., F. Ziparo et al. 2023). From the SFH modeled from JWST spectrophotometry, it is evident that many of the massive quiescent galaxies at $z \gtrsim 4$ are expected to be massive ($M_{\text{star}} \gtrsim 10^9 M_{\odot}$) star-forming ($\text{SFR} \gtrsim 10 M_{\odot} \text{yr}^{-1}$) galaxies at $z \sim 12$, matching the observables of the “blue monsters” at this epoch. The in-

ferred SFH of these early quiescent galaxies typically peak at $z \simeq 6 - 8$, with $\text{SFR} \gtrsim 100 M_{\odot} \text{yr}^{-1}$.

We find that the stellar mass and SFR of NIRCcam-dark DSFGs at $z \sim 7$ exactly match the starburst progenitors of massive quiescent galaxies at $z \sim 4$ (Figure 3). The compact sizes of their dust continuum emission (and therefore the molecular gas reservoir; $R_{\text{e,circ}} \sim 1 \text{ kpc}$) also resemble the compact stellar sizes of massive quiescent galaxies at $z \sim 4$ ($R_{\text{e,circ}} \lesssim 1 \text{ kpc}$; e.g., Z. Ji et al. 2024b). We therefore argue that NIRCcam-dark DSFGs are likely the progenitors of $z \sim 4$ massive quiescent galaxies and descendants of $z > 10$ “blue monsters”, or at least representing one viable intermediate galaxy population that can bridge the two massive galaxy populations before and after the EoR.

From cosmological simulations, it is also clear that the progenitors of $z \gtrsim 4$ massive quiescent galaxies should be massive gas-rich starburst galaxies at $z \sim 7$, matching the M_{star} and SFR of NIRCcam-dark galaxies in our sample (e.g., see the SFHs in Figure 3 simulated by FLARES, C. C. Lovell et al. 2023; IllustrisTNG, A. Pillepich et al. 2018; D. Nelson et al. 2019, see also A. I. Hartley et al. 2023; THESAN, R. Kannan et al. 2022; H. G. Chittenden et al. 2025).

However, we also note that many starburst galaxies with $\text{SFR} \gtrsim 100 M_{\odot} \text{yr}^{-1}$ at $z \sim 7$ may quench at later epochs (e.g., $z \sim 3$ from TNG100), possibly depending on the quenching physical mechanisms. The obscuration of star-

bursts at $z \sim 7$ also depends on complicated physics of dust production (e.g., A. Leńiewska & M. J. Michałowski 2019; C. R. Choban et al. 2025), geometry and sometimes viewing angles (R. K. Cochrane et al. 2024), many of which are not clear from either observational or theoretical perspectives. Specifically, the observed high dust-to-stellar mass ratio $\log(M_{\text{dust}}/M_{\text{star}}) \sim -2.3 \pm 0.5$ as observed for the two galaxies are perhaps particularly interesting. The observed $M_{\text{dust}}/M_{\text{star}}$ approaches the expectation from the “maximal dust model” at $z \sim 7$ through core-collapse supernovae dust production by P. Dayal et al. (2022), and match the G. Popping et al. (2017) model prediction at solar metallicity. Nevertheless, future deeper JWST imaging observations, in particular with multi-band MIRI imaging, are needed to provide tighter constraints on the M_{star} of the two objects and thus models of dust production (and destruction) for massive starburst galaxies in the EoR.

4.2. The number density of NIRC*am*-dark starbursts

To assess whether NIRC*am*-dark starbursts are possible progenitors of $z \gtrsim 4$ massive quiescent galaxies and descendants of $z > 10$ blue monsters, we analyze the number densities of these galaxy populations. The number density of massive quiescent galaxies at $z \gtrsim 4$ has been observed at $n \simeq 10^{-5} - 3 \times 10^{-5} \text{ Mpc}^{-3}$ (e.g., A. C. Carnall et al. 2023b; F. Valentino et al. 2023; A. S. Long et al. 2024b; W. M. Baker et al. 2025). On the other hand, JWST also measures the number density of luminous Lyman-break galaxies (absolute UV magnitude $M_{\text{UV}} \sim -21$, corresponding to a SFR $\sim 10 M_{\odot} \text{ yr}^{-1}$) at $z \sim 12$ as $n \sim 10^{-5} \text{ Mpc}^{-3}$ (e.g., C. T. Donnan et al. 2024; S. L. Finkelstein et al. 2024; B. Robertson et al. 2024; Y. Harikane et al. 2025; R. P. Naidu et al. 2025; L. Whitler et al. 2025). Therefore, if the abundance of NIRC*am*-dark DSFGs is also found to be $\sim 10^{-5} \text{ Mpc}^{-3}$, it would provide strong evidence to the evolutionary connection.

However, it is not easy to constrain the number density of NIRC*am*-dark galaxies because they are selected as companions of luminous quasars. Luminous quasars at $z \gtrsim 6$ are now confirmed to generally reside in massive dark matter halos thanks to JWST/NIRC*am* observations, in particularly with WFSS (e.g., D. Kashino et al. 2023; F. Wang et al. 2023; A.-C. Eilers et al. 2024; J. B. Champagne et al. 2025; M. Pudoka et al. 2025). Through the galaxy auto-correlation function, quasar-galaxy cross-correlation function and comparison with dark-matter-only simulations, the host halo masses of quasars are measured as $\log(M_{\text{halo}}) \gtrsim 12.30$ from the EIGER survey (six quasars at $z \sim 6$; A.-C. Eilers et al. 2024) and similarly with the ASPIRE survey (25 quasars at $z \simeq 6.5 - 6.8$; F. Wang et al. in prep.). Such massive halos are rare at $z \sim 6.6$ ($n < 10^{-7} \text{ Mpc}^{-3}$ based on the halo mass function, HMF model of S. G. Murray et al. 2013), although the number density is still much higher than that of quasars at this epoch ($n = 0.39 \pm 0.11 \text{ Gpc}^{-3}$; F. Wang et al. 2019).

E. Pizzati et al. (2024) developed an empirical quasar population model that successfully reproduces the clustering properties and luminosity functions (LF) of quasars based on

N-body simulations. Following this model, the luminosity of a quasar (or galaxy) is dependent on the halo mass, and the probability distribution function that a halo could host a detectable quasar (or galaxy), $P(M_{\text{halo}})$, can be approximated as a Gaussian function:

$$P(M_{\text{halo}}) = P_{\text{max}} \exp\left\{-\frac{[\log(M_{\text{halo}}/M_c)]^2}{2\sigma_m^2}\right\} \quad (1)$$

where P_{max} is the maximum likelihood of halo occupation, M_c is the characteristic halo mass, and σ_m is the mass dispersion. Taking the HMF at $z = 6.6$ (S. G. Murray et al. 2013) and the shape of quasar-host HMF (RMS of M_{halo}) inferred by E. Pizzati et al. (2024) for EIGER quasars (A.-C. Eilers et al. 2024), we reproduce the observed quasar number density at $z \sim 6.6$ with the parameter set $P_{\text{max}} = 0.02$, $\log(M_c/M_{\odot}) = 12.73$, $\sigma_m = 0.22$, and the resultant quasar host HMF is shown as the solid red line in Figure 4 (left panel). At the median $\log(M_{\text{halo}}/M_{\odot}) \sim 12.3$ of quasars, the fraction of halos that host a detectable quasar is very low ($\sim 3 \times 10^{-3}$).

Quasars are already rare objects residing in these massive halos, which likely indicates a low duty cycle in the UV-bright phase ($f_{\text{duty}} \lesssim 1\%$; e.g., A.-C. Eilers et al. 2024; E. Pizzati et al. 2024; F. Wang et al. in prep.). With ASPIRE, we identify two NIRC*am*-dark galaxies in 25 massive halo environments at $z \simeq 6.5 - 6.8$. Therefore, we conclude that the occurrence rate of NIRC*am*-dark galaxies ($f = 2/25 = 0.08^{+0.10}_{-0.05}$; error from Poisson statistics) must be much higher than that of the quasars, otherwise we would not be able to identify any NIRC*am*-dark galaxies with ASPIRE.

We explore the possible halo occupation models of NIRC*am*-dark galaxies in Figure 4 (left panel). The first model, dubbed “heavy model”, assumes that NIRC*am*-dark galaxies share the same halo characteristics (M_c and σ_m , Equation 1) but with much larger P_{max} and thus higher occurrence rate. We note that the large halo mass of a quasar also implies a virial radius $R_{200} \sim 50$ proper kpc, large enough to encompass the observed NIRC*am*-dark companions. We simulate the M_{halo} mass distribution of quasars from the aforementioned quasar host HMF, apply $P(M_{\text{halo}})$ and match the observed NIRC*am*-dark occurrence rate as observed by ASPIRE. We obtain $P_{\text{max}} = 0.37^{+0.46}_{-0.23}$ from this heavy model, suggesting a high occupation fraction of NIRC*am*-dark galaxies in the most massive halos at this epoch. According to this model, the predicted number density of NIRC*am*-dark galaxies is $n = 8^{+10}_{-5} \times 10^{-9} \text{ Mpc}^{-3}$, about $20\times$ of that of UV-bright quasars but still much lower than that of $z \gtrsim 4$ massive quiescent galaxies or $z > 10$ blue monsters (Figure 4, right panel).

We also test an alternative model, dubbed “light model”, in which the occupation fraction of NIRC*am*-dark galaxies is constant above certain M_{halo} threshold. Based on TNG100, we find that most of the $z \sim 6.5$ halos that host galaxies at SFR $> 50 M_{\odot} \text{ yr}^{-1}$ have a “cutoff” halo masses at $\log(M_{\text{halo}}/M_{\odot}) \geq 11.4$, and thus we adopt the threshold. The halo occupation fraction is therefore the observed

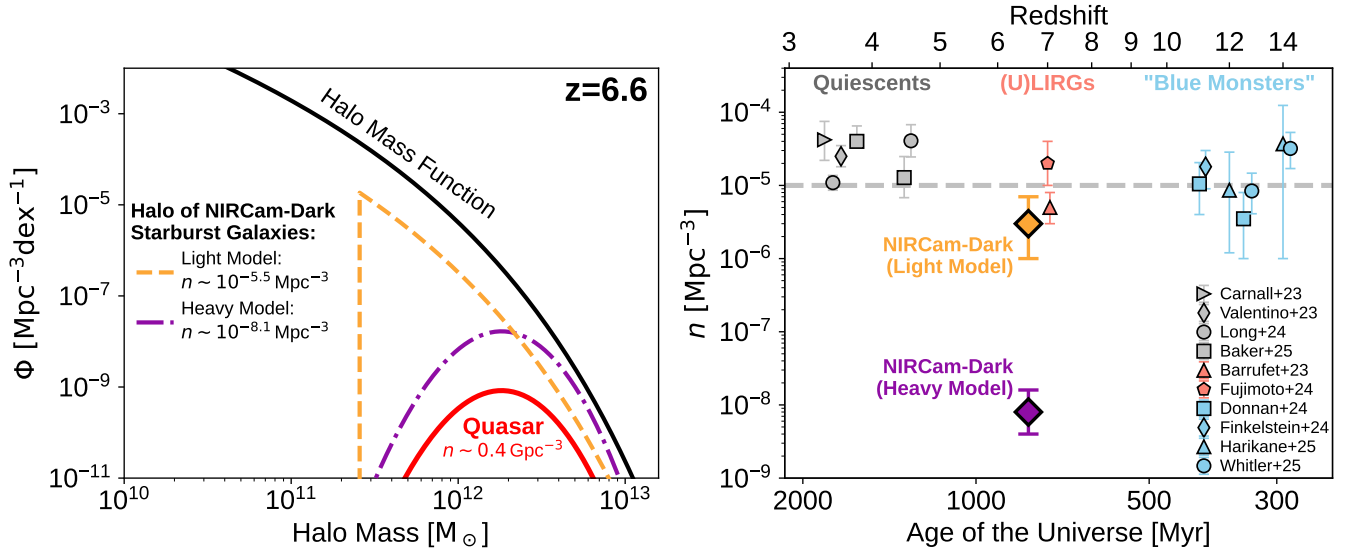


Figure 4. The number density constraint of NIRCcam-dark galaxies. **Left:** The host halo mass function models of NIRCcam-dark starburst galaxies at $z = 6.6$. We consider two models for their host mass distribution, including a light model (dashed orange line) and a heavy model (dashed-dotted purple line; Section 4.2). These two models predict completely different number densities of NIRCcam-dark galaxies, while both of them match the existing observations. For comparison we show the quasar host HMF (red) and overall HMF (black) at the same redshift. **Right:** Comparison of the number densities with massive quiescent galaxies at $z \sim 4$ (A. C. Carnall et al. 2023b; F. Valentino et al. 2023; A. S. Long et al. 2024b; W. M. Baker et al. 2025), (U)LIRGs at $z \sim 7$ (L. Barrufet et al. 2023; S. Fujimoto et al. 2024, see Section 4.2 for details) and “blue monsters” at $z > 10$ (C. T. Donnan et al. 2024; S. L. Finkelstein et al. 2024; Y. Harikane et al. 2025; L. Whittler et al. 2025, computed from their measured UVLFs in the brightest bins, typically at $M_{UV} \sim -21$ mag). The derived number densities of NIRCcam-dark galaxies based on the light and heavy halo occupation model are shown as orange and purple diamonds, respectively.

NIRCcam-dark occurrence rate ($0.08^{+0.10}_{-0.05}$). At above the halo mass threshold, the expected number density of NIRCcam-dark galaxy is $n = 3^{+4}_{-2} \times 10^{-6} \text{ Mpc}^{-3}$. Under such a light model, the number density of NIRCcam-dark galaxies will be about $30^{+40}_{-20}\%$ of those of $z \gtrsim 4$ massive quiescent galaxies and $z > 10$ blue monsters (Figure 4, right panel).

We conclude that the number density of NIRCcam-dark galaxies at $z \sim 7$ remains highly unconstrained: it may be as low as $n \sim 10^{-8.1} \text{ Mpc}^{-3}$, but could also be as high as $\sim 10^{-5.5} \text{ Mpc}^{-3}$. From an abundance-matching perspective, this implies that a substantial fraction of the progenitors of massive quiescent galaxies at $z \gtrsim 4$, as well as the descendants of $z > 10$ blue monsters, could be NIRCcam-dark at $z \sim 7$. This hypothesis will need to be tested through both observations and simulations, including studies of dust production and obscuration mechanisms.

We also emphasize that our models assume independent halo occupations for quasars and NIRCcam-dark galaxies. If the two populations are correlated or anti-correlated, the number density estimates could be even more uncertain. We argue that the large M_{dust} , high A_v and high $M_{\text{dust}}/M_{\text{star}}$ of NIRCcam-dark galaxies imply efficient dust production over extended period (e.g., ~ 300 Myr; Y. Tamura et al. 2019)—significantly longer than both the Salpeter timescale of quasar and the major merger timescale predicted by cosmological simulations, which are ~ 50 Myr at this epoch (e.g., G. F. Snyder et al. 2017). Therefore, while interactions between quasar host galaxies and NIRCcam-dark galax-

ies may occur in the present or upcoming epoch, their halo occupations can still be treated as independent.

We also note that, according to the IRLF at $z \sim 7$ from S. Fujimoto et al. (2024), the integrated number density of $z \sim 7$ DSFGs with $\text{SFR} \simeq 50\text{--}500 \text{ M}_{\odot} \text{ yr}^{-1}$ is $n \sim 2 \times 10^{-5} \text{ Mpc}^{-3}$. This exceeds the number density of $n \sim 5 \times 10^{-6} \text{ Mpc}^{-3}$ derived from the $z \sim 7$ IRLF of L. Barrufet et al. (2023) over the same SFR range, which is based on REBELS-ALMA observations of the L_{IR} of UV-luminous galaxies and the UVLF as a proxy. Although caution should be taken given the substantial uncertainties in the IRLFs at $z > 7$, if NIRCcam-dark galaxies follow a “light model” of halo occupation, they may represent a substantial fraction (likely $\gtrsim 30\%$) of the (U)LIRG population and the obscured cosmic star formation rate density at $z \sim 7$. These galaxies are likely to be missed in most blank-field surveys due to their rarity and faintness in the near-IR. Indeed, the NIRCcam-dark fraction of quasar companion DSFGs detected by ASPIRE-ALMA is $2/6 = 33\%$, consistent with the fraction inferred above.

Finally, we note that NIRCcam-dark galaxies at $z \simeq 6 - 7$ may reside above the detection limit of wide ALMA surveys like GOODS-ALMA 2.0 (C. Gómez-Guijarro et al. 2022, $\sim 72 \text{ arcmin}^2$ down to $S_{1.1\text{mm}} \sim 0.34 \text{ mJy}$), but the expected number of detections is only $N \sim 0.5$ (and $N \sim 1.5$ for general DSFGs with $\text{SFR} \simeq 50 - 500 \text{ M}_{\odot} \text{ yr}^{-1}$). Therefore, a non-detection so far is fully consistent with the cosmic shot noise.

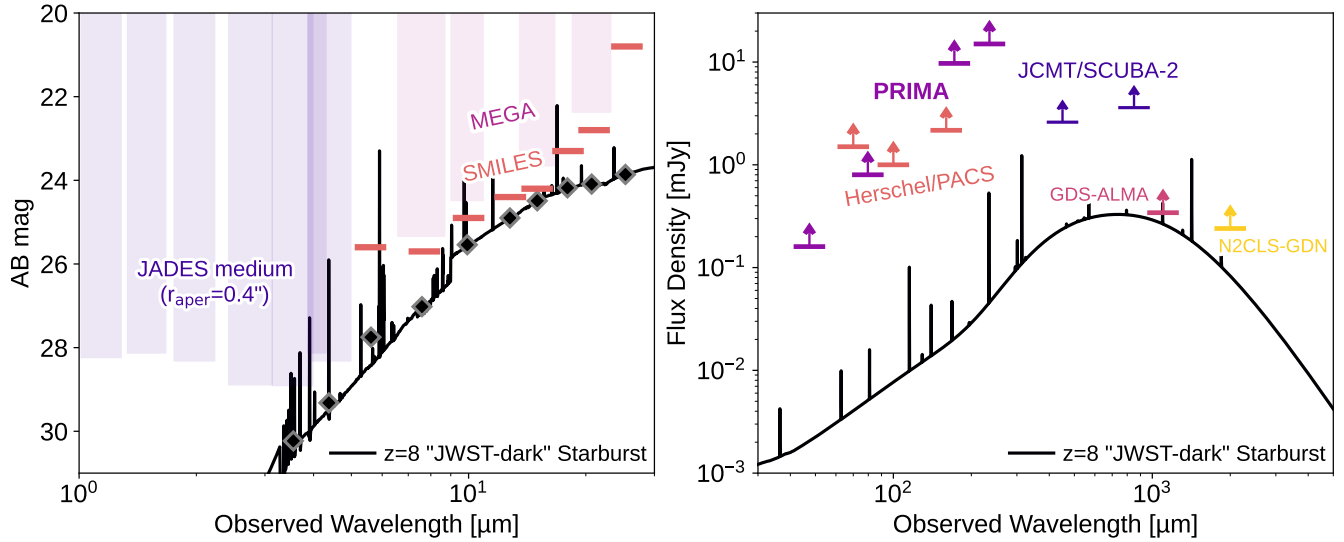


Figure 5. The best-fit SED model of J0305m3150.C05 but redshifted to $z = 8$ and scaled to a SFR of $60 M_{\odot} \text{ yr}^{-1}$ (solid black lines). **Left:** the near-to-mid-infrared SED compared with the 5σ detection limits of representative JWST NIRCcam and MIRI imaging surveys, including JADES-medium at $1\text{--}5 \mu\text{m}$ (indigo; D. J. Eisenstein et al. 2023; F. D’Eugenio et al. 2025), SMILES at $5\text{--}25 \mu\text{m}$ (coral; G. H. Rieke et al. 2024; S. Alberts et al. 2024) and MEGA at $7\text{--}21 \mu\text{m}$ (purple; B. E. Backhaus et al. 2025). The gray-edged diamonds denote the brightnesses of the SED template in the corresponding JWST bands. **Right:** the far-infrared SED compared with the 5σ detection limits of Herschel/PACS at $70\text{--}160 \mu\text{m}$ (from the PEP survey; D. Lutz et al. 2011), the planned PRIMA/PRIMAger at $47\text{--}235 \mu\text{m}$ (including realistic confusion noise; J. M. S. Donnellan et al. 2024), JCMT/SCUBA-2 at 450 and $850 \mu\text{m}$ (e.g., C.-F. Lim et al. 2020), the GOODS-ALMA v2.0 survey at 1.1 mm (C. Gómez-Guijarro et al. 2022), the N2CLS survey in the GOODS-N field at $2 \mu\text{m}$ (L. Bing et al. 2023). Such a predicted “JWST-dark” galaxy at $z = 8$, if it exists, will remain undetected with all aforementioned surveys or planned facilities.

4.3. Multi-wavelength detectability

We further investigate the multi-wavelength detectability of NIRCcam-dark galaxies in wide-area infrared and millimeter surveys, to assess whether NIRCcam-dark galaxies are indeed a population missed by most of the high-redshift galaxy surveys obtained so far. The NIRCcam imaging depth of the ASPIRE survey is slightly shallower than the average depth of CEERS (S. L. Finkelstein et al. 2025), but is deeper than wider surveys like COSMOS-Web (C. M. Casey et al. 2023) and COSMOS-3D (JWST-GO-5893, PI: Kakiichi, K.; cf. X. Lin et al. 2025). At $z = 6.6$, the F356W brightness of J1526m2050.C02 (and likely J0305m3150.C05) can be detected by surveys like JADES-medium (D. J. Eisenstein et al. 2023; F. D’Eugenio et al. 2025, $\gtrsim 125 \text{ arcmin}^2$) down to ~ 29 AB mag with aperture size of $r = 0''.4$ (5σ).

Indeed, a NIRCcam-dark MIRI-only source was reported by P. G. Pérez-González et al. (2024) in the HUDF, and two heavily reddened NIRCcam-faint MIRI sources at photometric redshifts $z \sim 8$ have also been reported by H. B. Akins et al. (2023) in the COSMOS field. We note that these MIRI sources are rather compact, making them resembling reddened AGNs instead of DSFGs (similar to *Virgil* at $z = 6.6$, P. Rinaldi et al. 2025 and other HST-dark MIRI sources at $z > 6$ in C. C. Williams et al. 2024). NIRCcam-dark ALMA-only sources have also been reported by S. Fujimoto et al. (2023) through a deep 1.2-mm survey in the Abell 2744 lensing cluster field and T. J. L. C. Bakx et al.

(2024) as [C II] emitters in quasar fields (B. P. Venemans et al. 2020). However, we caution the relatively low S/N of these sources ($\lesssim 5$ for continuum and $\lesssim 6$ for emission-line scan within the ALMA spectral cubes). Further deeper imaging and spectroscopic confirmation are necessary to confirm the fidelity, redshifts and nature of these sources. We also remark that SPT0311-58, an extraordinarily luminous lensed DSFG at $z = 6.90$ (M. L. Strandet et al. 2017) can be classified as a NIRCcam-dark galaxy according to the MIRI $10\text{-}\mu\text{m}$ detection (J. Álvarez-Márquez et al. 2023) but non-detection at $\leq 5 \mu\text{m}$ with NIRSpec (S. Arribas et al. 2024), although the contamination from the foreground lens may complicate the interpretation.

At higher redshifts, the IR detectability of NIRCcam-dark galaxies (and DSFGs in general) may rapidly decrease because of the surface brightness dimming and K correction. Figure 5 shows the SED model of J0305m3150.C05 but redshifted to $z = 8$, scaled to a SFR of $60 M_{\odot} \text{ yr}^{-1}$. The existence of galaxies with such SFR at $z \sim 8$ is expected from the SFH of massive quiescent galaxies at $z \gtrsim 4$, while most of the galaxies at $z \gtrsim 8$ are observed at $M_{\text{UV}} \lesssim -22$ mag (one of the brightest is EGSz8p7 at $z=8.68$; A. Zitrin et al. 2015; S. L. Finkelstein et al. 2024; Y. Harikane et al. 2024), corresponding to unobscured SFR $\lesssim 30 M_{\odot} \text{ yr}^{-1}$. In other words, dust-obscured star-forming galaxies at $z > 8$ are clearly missing from the current JWST observations (or at least spectroscopic confirmation); one example of such a galaxy is MACS0416_Y1 at $z = 8.31$ where the majority

of the SFR is dust-obscured (Y. Tamura et al. 2019). We also note that MACS0416.Y1 likely resides in a complex galaxy overdensity (and thus massive halo) at $z \simeq 8.3 - 8.5$ in and around the MACS0416 cluster field (Z. Ma et al. 2024; Y. Fudamoto et al. 2025).

We compare with the detection limits of multiple surveys at the JWST wavelengths and also far-infrared to millimeter wavelengths. At NIRCam wavelengths, the $z = 8$ galaxy template will fall below the 5σ detection limit of wide surveys like JADES-medium (assuming $r = 0''.4$ aperture), not to mention shallower surveys like CEERS (S. L. Finkelstein et al. 2025), PRIMER (JWST-GO-1837, PI: J. Dunlop) and COSMOS-web (C. M. Casey et al. 2023). At MIRI wavelengths, the galaxy will fall below the 5σ detection limit of wide surveys like SMILES (S. Albers et al. 2024; G. H. Rieke et al. 2024) and MEGA (B. E. Backhaus et al. 2025), which is also the case for other wide surveys including PRIMER, COSMOS-Web and MEOW (JWST-GO-5407, PI: G. Leung). In these existing wide-area surveys, these galaxies will even appear “JWST-dark”.

In the far-IR, by considering realistic confusion noise limit, such a “JWST-dark” galaxy at $z = 8$ will fall below the detection limit of Herschel/PACS and SPIRE at $70-500 \mu\text{m}$ (e.g., H. T. Nguyen et al. 2010; D. Lutz et al. 2011), JCMT/SCUBA-2 at 450 and $850 \mu\text{m}$ (e.g., C.-F. Lim et al. 2020) and even the planned PRIMA/PRIMAger at $47-235 \mu\text{m}$ (C. T. Donnan et al. 2024). It will also fall below the confusion limit of single-dish millimeter facilities like IRAM30m/NIKA2 at 1.2 and 2 mm (e.g., L. Bing et al. 2023), and also wide-field ALMA Band-6 continuum surveys like GOODS-ALMA v2.0 ($\sim 72 \text{ arcmin}^2$; C. Gómez-Guijarro et al. 2022), not to mention shallower surveys like (Ex)-MORA (C. M. Casey et al. 2021; A. S. Long et al. 2024a) and Cycle-10 large program CHAMPS (2023.1.00180.L; PI: A. Faisst). Therefore, we conclude that current wide-area extragalactic surveys are generally insensitive to “JWST-dark” galaxies at $z \sim 8$.

If “JWST-dark” galaxies do exist at such an early epoch, how could we detect and confirm these galaxies? In fact, from Figure 5, it is evident that the galaxy brightness is not far from the current detection limits in certain bands, specifically NIRCam F444W, MIRI F1000W~F1500W and ALMA Band-6/7. With a few hours of JWST integration and probably less than an hour of ALMA integration (especially with the upcoming wideband sensitivity upgrade; J. Carpenter et al. 2023), these “JWST-dark” galaxies can be detected and studied with JWST and ALMA. We argue that the key is to locate the targets prior to the MIRI and ALMA follow-up observations with relatively small FoVs. This requires the selection of massive dark matter halos at $z \sim 8$ in the first place (similar to the ASPIRE approach), possibly through wide-field NIRCam photometry and slitless spectroscopy of emission-line galaxies at $z \gtrsim 8$ as protocluster tracers (e.g., J. M. Helton et al. 2024; Z. Ma et al. 2024; Y. Fudamoto et al. 2025; Q. Li et al. 2025).

Through the JWST Cycle-3 large NIRCam WFSS campaigns like SAPPHIRES (F. Sun et al. 2025b), NEXUS (Y.

Shen et al. 2024), COSMOS-3D, and POPPIES (JWST-GO-5398, PI: Kartaltepe, J. & Rafelski, M.), more protocluster candidates will be selected at $z \gtrsim 8$. The pure-parallel NIRCam WFSS programs (e.g., SAPPHIRES and POPPIES) are particularly important because they could overcome the strong cosmic variance through multiple independent sight-lines (see F. Sun et al. 2025b). Combined with pointed NIRCam WFSS observations of massive galaxies (e.g., JWST-GO-6480, PI: Schouws, S.), these surveys will further unveil the existence of NIRCam-dark or even JWST-dark galaxies, measuring their clustering properties and halo occupation fraction (e.g., differentiating the light versus heavy model in Section 4.2), and thus providing key insights into the evolution history of massive galaxies and the dust-obscured cosmic star-formation history deeply into the EoR.

5. SUMMARY

We present a study of two NIRCam-dark dusty star-forming galaxies at $z = 6.6$. These two galaxies are identified as companions to quasars through the ASPIRE JWST and ALMA survey, which targeted 25 UV-luminous quasars and their environments at $z \simeq 6.5 - 6.8$. The main results are summarized as follows:

1. We securely detect ($> 8\sigma$) the dust continuum emissions of the two galaxies through multiple ALMA bands, and the redshifts are confirmed through [C II] line spectroscopy, placing them as quasar companions at $z = 6.6$. In contrast to the vast majority of DSFGs found through ALMA surveys in blank fields, these two sources are extraordinarily faint at the NIRCam wavelengths ($F_{356W} > 28.0 \text{ mag}$ for J0305m3150.C05 and $26.5 \pm 0.1 \text{ mag}$ for J1526m2050.C02). We refer to them as NIRCam-dark galaxies because of their near-IR faintness ($S_{3.6 \mu\text{m}}/S_{1.2 \text{ mm}} < 10^{-4}$).
2. We obtain physical SED modeling of the two NIRCam-dark galaxies. These galaxies are undergoing starbursts ($\text{SFR} \simeq 80 - 250 M_{\odot} \text{ yr}^{-1}$), appear more obscured than Arp 220 (whole galaxy) and optically faint DSFGs at $z \sim 3$ selected through the ALESS survey (E. da Cunha et al. 2015). The stellar masses are poorly constrained ($\log(M_{\text{star}}/M_{\odot}) \simeq 10.0 - 10.5$ with an error of 0.5 dex) because of the near-IR faintness.
3. Given the mass, SFR and redshifts, we show that the NIRCam-dark galaxies are viable progenitors of massive quiescent galaxies at $z \gtrsim 4$ according to their star formation histories. They could also be the descendants of certain UV-luminous galaxies at $z > 10$ (“blue monsters”), bridging the two populations of massive galaxies before and after the epoch of reionization through an evolutionary perspective.
4. We show that the number density of NIRCam-dark galaxies is highly unconstrained from biased surveys

like ASPIRE ($n \simeq 10^{-8.1} \sim 10^{-5.5} \text{ Mpc}^{-3}$). However, based on a light halo occupation model that could match the ASPIRE observations, the number density of NIRCam-dark galaxies at $z \sim 6.6$ could reach $n = 3_{-2}^{+4} \times 10^{-6} \text{ Mpc}^{-3}$. If true, this will equal to $\sim 30\%$ of the number density of massive quiescent galaxies at $z \gtrsim 4$ and blue monsters at $z > 10$, suggesting a substantial contribution to the dust-obscured cosmic star-formation rate density at $z \sim 7$ through the “NIRCam-dark” population.

- From the SFH of massive quiescent galaxies at $z \gtrsim 4$, galaxies with similar SFR should also exist at $z \sim 8$. If a substantial fraction of them share a similar SED to that of J0305m3150.C05, these galaxies will reside below the detection limits of most wide-area JWST, ALMA and other single-dish (sub)-millimeter surveys obtained so far, and thus remaining “JWST-dark”. To study these “JWST-dark” galaxies, large-area JWST/NIRCam imaging and WFSS surveys of early galaxy protoclusters ($z \gtrsim 8$) are essential. Deep JWST and ALMA follow-up observations of these protoclusters will likely detect such galaxies, offering deep insight to the dust-obscured cosmic star formation in the Epoch of Reionization.

ACKNOWLEDGMENT

F.S. acknowledges funding from JWST/NIRCam contract to the University of Arizona, NAS5-02105 and support for JWST program #2883, 4924, 5105, 6434 provided by NASA through grants from the Space Telescope Science Institute, which is operated by the Association of Universities for Research in Astronomy, Inc., under NASA contract NAS 5-03127. F.W. acknowledges support from NSF award AST-2513040. D.J.E.’s contributions were supported by JWST/NIRCam contract to the University of Arizona, NAS5-02015, and as a Simons Foundation Investigator. S.E.I.B. is supported by the Deutsche Forschungsgemeinschaft (DFG) under Emmy Noether grant number BO 5771/1-1. L.C. acknowledges support by grant PIB2021-127718NB-100 from the Spanish Ministry of Science and Innovation/State Agency of Re-

search MCIN/AEI/10.13039/501100011033 and by “ERDF A way of making Europe” C.M. acknowledges support from Fondecyt Iniciacion grant 11240336 and the ANID BASAL project FB210003. F.S. thanks Tiger Hsiao and James Trussler for helpful discussions.

This paper makes use of the following ALMA data: ADS/JAO.ALMA#2017.1.00139.S, 2017.1.01532.S, 2019.1.00147.S, 2021.1.00443.S and 2022.1.01077.L. ALMA is a partnership of ESO (representing its member states), NSF (USA) and NINS (Japan), together with NRC (Canada), MOST and ASIAA (Taiwan), and KASI (Republic of Korea), in cooperation with the Republic of Chile. The Joint ALMA Observatory is operated by ESO, AUI/NRAO and NAOJ. The National Radio Astronomy Observatory is a facility of the National Science Foundation operated under cooperative agreement by Associated Universities, Inc.

This work is based on observations made with the NASA/ESA/CSA James Webb Space Telescope. The data were obtained from the Mikulski Archive for Space Telescopes at the Space Telescope Science Institute, which is operated by the Association of Universities for Research in Astronomy, Inc., under NASA contract NAS 5-03127 for JWST. These observations are associated with program #2078. Support for program #2078 was provided by NASA through a grant from the Space Telescope Science Institute, which is operated by the Association of Universities for Research in Astronomy, Inc., under NASA contract NAS 5-03127.

AUTHOR CONTRIBUTIONS

FS led the ALMA data processing, analyses of the targets and the paper writing. JY led the NIRCam imaging data processing. FW led the JWST and ALMA observing programs. All co-authors contributed to the scientific interpretation of the results and helped to write the manuscript.

Facilities: ALMA, JWST(NIRCam)

Software: ASTROPY (Astropy Collaboration et al. 2013, 2018), CASA (CASA Team et al. 2022), CIGALE (S. Noll et al. 2009; M. Boquien et al. 2019), JWST (H. Bushouse et al. 2023), PHOTUTILS (L. Bradley et al. 2024)

REFERENCES

- Akins, H. B., Casey, C. M., Allen, N., et al. 2023, ApJ, 956, 61, doi: [10.3847/1538-4357/acef21](https://doi.org/10.3847/1538-4357/acef21)
- Alberts, S., Lyu, J., Shivaee, I., et al. 2024, ApJ, 976, 224, doi: [10.3847/1538-4357/ad7396](https://doi.org/10.3847/1538-4357/ad7396)
- Algera, H. S. B., Inami, H., Oesch, P. A., et al. 2023, MNRAS, 518, 6142, doi: [10.1093/mnras/stac3195](https://doi.org/10.1093/mnras/stac3195)
- Álvarez-Márquez, J., Crespo Gómez, A., Colina, L., et al. 2023, A&A, 671, A105, doi: [10.1051/0004-6361/202245400](https://doi.org/10.1051/0004-6361/202245400)
- Aravena, M., Boogaard, L., González-López, J., et al. 2020, arXiv e-prints, arXiv:2006.04284. <https://arxiv.org/abs/2006.04284>
- Arrabal Haro, P., Dickinson, M., Finkelstein, S. L., et al. 2023, Nature, 622, 707, doi: [10.1038/s41586-023-06521-7](https://doi.org/10.1038/s41586-023-06521-7)
- Arribas, S., Perna, M., Rodríguez Del Pino, B., et al. 2024, A&A, 688, A146, doi: [10.1051/0004-6361/202348824](https://doi.org/10.1051/0004-6361/202348824)
- Astropy Collaboration, Robitaille, T. P., Tollerud, E. J., et al. 2013, A&A, 558, A33, doi: [10.1051/0004-6361/201322068](https://doi.org/10.1051/0004-6361/201322068)
- Astropy Collaboration, Price-Whelan, A. M., Sipőcz, B. M., et al. 2018, AJ, 156, 123, doi: [10.3847/1538-3881/aabc4f](https://doi.org/10.3847/1538-3881/aabc4f)
- Backhaus, B. E., Kirkpatrick, A., Yang, G., et al. 2025, arXiv e-prints, arXiv:2503.19078, doi: [10.48550/arXiv.2503.19078](https://doi.org/10.48550/arXiv.2503.19078)

- Baker, W. M., Lim, S., D'Eugenio, F., et al. 2025, MNRAS, 539, 557, doi: [10.1093/mnras/staf475](https://doi.org/10.1093/mnras/staf475)
- Bakx, T. J. L. C., Algera, H. S. B., Venemans, B., et al. 2024, MNRAS, 532, 2270, doi: [10.1093/mnras/stae1613](https://doi.org/10.1093/mnras/stae1613)
- Barrufet, L., Oesch, P. A., Bouwens, R., et al. 2023, MNRAS, 522, 3926, doi: [10.1093/mnras/stad1259](https://doi.org/10.1093/mnras/stad1259)
- Bing, L., Béthermin, M., Lagache, G., et al. 2023, A&A, 677, A66, doi: [10.1051/0004-6361/202346579](https://doi.org/10.1051/0004-6361/202346579)
- Boogaard, L. A., Gillman, S., Melinder, J., et al. 2024, ApJ, 969, 27, doi: [10.3847/1538-4357/ad43e5](https://doi.org/10.3847/1538-4357/ad43e5)
- Boquien, M., Burgarella, D., Roehlly, Y., et al. 2019, A&A, 622, A103, doi: [10.1051/0004-6361/201834156](https://doi.org/10.1051/0004-6361/201834156)
- Bouwens, R. J., Smit, R., Schouws, S., et al. 2022, ApJ, 931, 160, doi: [10.3847/1538-4357/ac5a4a](https://doi.org/10.3847/1538-4357/ac5a4a)
- Bradley, L., Sipőcz, B., Robitaille, T., et al. 2024, 1.12.0 Zenodo, doi: [10.5281/zenodo.10967176](https://doi.org/10.5281/zenodo.10967176)
- Bruzual, G., & Charlot, S. 2003, MNRAS, 344, 1000, doi: [10.1046/j.1365-8711.2003.06897.x](https://doi.org/10.1046/j.1365-8711.2003.06897.x)
- Bunker, A. J., Saxena, A., Cameron, A. J., et al. 2023, A&A, 677, A88, doi: [10.1051/0004-6361/202346159](https://doi.org/10.1051/0004-6361/202346159)
- Bushouse, H., Eisenhamer, J., Dencheva, N., et al. 2023, 1.10.2 Zenodo, doi: [10.5281/zenodo.7829329](https://doi.org/10.5281/zenodo.7829329)
- Calzetti, D., Armus, L., Bohlin, R. C., et al. 2000, ApJ, 533, 682, doi: [10.1086/308692](https://doi.org/10.1086/308692)
- Carnall, A. C., McLure, R. J., Dunlop, J. S., et al. 2023a, Nature, 619, 716, doi: [10.1038/s41586-023-06158-6](https://doi.org/10.1038/s41586-023-06158-6)
- Carnall, A. C., McLeod, D. J., McLure, R. J., et al. 2023b, MNRAS, 520, 3974, doi: [10.1093/mnras/stad369](https://doi.org/10.1093/mnras/stad369)
- Carnall, A. C., Cullen, F., McLure, R. J., et al. 2024, MNRAS, 534, 325, doi: [10.1093/mnras/stae2092](https://doi.org/10.1093/mnras/stae2092)
- Carniani, S., Hainline, K., D'Eugenio, F., et al. 2024, Nature, 633, 318, doi: [10.1038/s41586-024-07860-9](https://doi.org/10.1038/s41586-024-07860-9)
- Carpenter, J., Brogan, C., Iono, D., & Mroczkowski, T. 2023, in Physics and Chemistry of Star Formation: The Dynamical ISM Across Time and Spatial Scales, ed. V. Ossenkopf-Okada, R. Schaaf, I. Breloy, & J. Stutzki, 304, doi: [10.48550/arXiv.2211.00195](https://doi.org/10.48550/arXiv.2211.00195)
- CASA Team, Bean, B., Bhatnagar, S., et al. 2022, PASP, 134, 114501, doi: [10.1088/1538-3873/ac9642](https://doi.org/10.1088/1538-3873/ac9642)
- Casey, C. M. 2012, MNRAS, 425, 3094, doi: [10.1111/j.1365-2966.2012.21455.x](https://doi.org/10.1111/j.1365-2966.2012.21455.x)
- Casey, C. M., Zavala, J. A., Manning, S. M., et al. 2021, ApJ, 923, 215, doi: [10.3847/1538-4357/ac2eb4](https://doi.org/10.3847/1538-4357/ac2eb4)
- Casey, C. M., Kartaltepe, J. S., Drakos, N. E., et al. 2023, ApJ, 954, 31, doi: [10.3847/1538-4357/acc2bc](https://doi.org/10.3847/1538-4357/acc2bc)
- Castellano, M., Napolitano, L., Fontana, A., et al. 2024, ApJ, 972, 143, doi: [10.3847/1538-4357/ad5f88](https://doi.org/10.3847/1538-4357/ad5f88)
- Chabrier, G. 2003, PASP, 115, 763, doi: [10.1086/376392](https://doi.org/10.1086/376392)
- Champagne, J. B., Wang, F., Zhang, H., et al. 2025, ApJ, 981, 113, doi: [10.3847/1538-4357/adb1bd](https://doi.org/10.3847/1538-4357/adb1bd)
- Chary, R., & Elbaz, D. 2001, ApJ, 556, 562, doi: [10.1086/321609](https://doi.org/10.1086/321609)
- Chen, C.-C., Smail, I., Swinbank, A. M., et al. 2015, ApJ, 799, 194, doi: [10.1088/0004-637X/799/2/194](https://doi.org/10.1088/0004-637X/799/2/194)
- Chittenden, H. G., Glazebrook, K., Nanayakkara, T., et al. 2025, arXiv e-prints, arXiv:2504.19696, doi: [10.48550/arXiv.2504.19696](https://doi.org/10.48550/arXiv.2504.19696)
- Choban, C. R., Salim, S., Kereš, D., Hayward, C. C., & Sandstrom, K. M. 2025, MNRAS, 537, 1518, doi: [10.1093/mnras/staf118](https://doi.org/10.1093/mnras/staf118)
- Cochrane, R. K., Anglés-Alcázar, D., Cullen, F., & Hayward, C. C. 2024, ApJ, 961, 37, doi: [10.3847/1538-4357/ad02f8](https://doi.org/10.3847/1538-4357/ad02f8)
- Connor, T., Bañados, E., Mazzucchelli, C., et al. 2020, ApJ, 900, 189, doi: [10.3847/1538-4357/abaab9](https://doi.org/10.3847/1538-4357/abaab9)
- da Cunha, E., Groves, B., Walter, F., et al. 2013, ApJ, 766, 13, doi: [10.1088/0004-637X/766/1/13](https://doi.org/10.1088/0004-637X/766/1/13)
- da Cunha, E., Walter, F., Smail, I. R., et al. 2015, ApJ, 806, 110, doi: [10.1088/0004-637X/806/1/110](https://doi.org/10.1088/0004-637X/806/1/110)
- Dayal, P., Ferrara, A., Sommovigo, L., et al. 2022, MNRAS, 512, 989, doi: [10.1093/mnras/stac537](https://doi.org/10.1093/mnras/stac537)
- de Graaff, A., Setton, D. J., Brammer, G., et al. 2025, Nature Astronomy, 9, 280, doi: [10.1038/s41550-024-02424-3](https://doi.org/10.1038/s41550-024-02424-3)
- De Rossi, M. E., Rieke, G. H., Shivaee, I., Bromm, V., & Lyu, J. 2018, ApJ, 869, 4, doi: [10.3847/1538-4357/aaebf8](https://doi.org/10.3847/1538-4357/aaebf8)
- Decarli, R., Walter, F., Venemans, B. P., et al. 2017, Nature, 545, 457, doi: [10.1038/nature22358](https://doi.org/10.1038/nature22358)
- D'Eugenio, F., Cameron, A. J., Scholtz, J., et al. 2025, ApJS, 277, 4, doi: [10.3847/1538-4365/ada148](https://doi.org/10.3847/1538-4365/ada148)
- Dey, A., Schlegel, D. J., Lang, D., et al. 2019, AJ, 157, 168, doi: [10.3847/1538-3881/ab089d](https://doi.org/10.3847/1538-3881/ab089d)
- Díaz-Santos, T., Armus, L., Charmandaris, V., et al. 2017, ApJ, 846, 32, doi: [10.3847/1538-4357/aa81d7](https://doi.org/10.3847/1538-4357/aa81d7)
- Donnan, C. T., McLure, R. J., Dunlop, J. S., et al. 2024, MNRAS, 533, 3222, doi: [10.1093/mnras/stae2037](https://doi.org/10.1093/mnras/stae2037)
- Donnellan, J. M. S., Oliver, S. J., Béthermin, M., et al. 2024, MNRAS, 532, 1966, doi: [10.1093/mnras/stae1539](https://doi.org/10.1093/mnras/stae1539)
- Dudzevičiūtė, U., Smail, I., Swinbank, A. M., et al. 2020, MNRAS, 494, 3828, doi: [10.1093/mnras/staa769](https://doi.org/10.1093/mnras/staa769)
- Dunlop, J. S., McLure, R. J., Biggs, A. D., et al. 2017, MNRAS, 466, 861, doi: [10.1093/mnras/stw3088](https://doi.org/10.1093/mnras/stw3088)
- Eilers, A.-C., Mackenzie, R., Pizzati, E., et al. 2024, ApJ, 974, 275, doi: [10.3847/1538-4357/ad778b](https://doi.org/10.3847/1538-4357/ad778b)
- Eisenstein, D. J., Willott, C., Alberts, S., et al. 2023, arXiv e-prints, arXiv:2306.02465, doi: [10.48550/arXiv.2306.02465](https://doi.org/10.48550/arXiv.2306.02465)
- Finkelstein, S. L., Leung, G. C. K., Bagley, M. B., et al. 2024, ApJL, 969, L2, doi: [10.3847/2041-8213/ad4495](https://doi.org/10.3847/2041-8213/ad4495)
- Finkelstein, S. L., Bagley, M. B., Arrabal Haro, P., et al. 2025, ApJL, 983, L4, doi: [10.3847/2041-8213/adbbd3](https://doi.org/10.3847/2041-8213/adbbd3)
- Franco, M., Elbaz, D., Béthermin, M., et al. 2018, A&A, 620, A152, doi: [10.1051/0004-6361/201832928](https://doi.org/10.1051/0004-6361/201832928)
- Fudamoto, Y., Oesch, P. A., Schouws, S., et al. 2021, Nature, 597, 489, doi: [10.1038/s41586-021-03846-z](https://doi.org/10.1038/s41586-021-03846-z)

- Fudamoto, Y., Helton, J. M., Lin, X., et al. 2025, arXiv e-prints, arXiv:2503.15597, doi: [10.48550/arXiv.2503.15597](https://doi.org/10.48550/arXiv.2503.15597)
- Fujimoto, S., Bezanson, R., Labbe, I., et al. 2023, arXiv e-prints, arXiv:2309.07834, doi: [10.48550/arXiv.2309.07834](https://doi.org/10.48550/arXiv.2309.07834)
- Fujimoto, S., Kohno, K., Ouchi, M., et al. 2024, ApJS, 275, 36, doi: [10.3847/1538-4365/ad5ae2](https://doi.org/10.3847/1538-4365/ad5ae2)
- Gaia Collaboration, Vallenari, A., Brown, A. G. A., et al. 2023, A&A, 674, A1, doi: [10.1051/0004-6361/202243940](https://doi.org/10.1051/0004-6361/202243940)
- Glazebrook, K., Nanayakkara, T., Schreiber, C., et al. 2024, Nature, 628, 277, doi: [10.1038/s41586-024-07191-9](https://doi.org/10.1038/s41586-024-07191-9)
- Gómez-Guijarro, C., Elbaz, D., Xiao, M., et al. 2022, A&A, 658, A43, doi: [10.1051/0004-6361/202141615](https://doi.org/10.1051/0004-6361/202141615)
- González-López, J., Novak, M., Decarli, R., et al. 2020, arXiv e-prints, arXiv:2002.07199. <https://arxiv.org/abs/2002.07199>
- Harikane, Y., Nakajima, K., Ouchi, M., et al. 2024, ApJ, 960, 56, doi: [10.3847/1538-4357/ad0b7e](https://doi.org/10.3847/1538-4357/ad0b7e)
- Harikane, Y., Ouchi, M., Inoue, A. K., et al. 2020, ApJ, 896, 93, doi: [10.3847/1538-4357/ab94bd](https://doi.org/10.3847/1538-4357/ab94bd)
- Harikane, Y., Inoue, A. K., Ellis, R. S., et al. 2025, ApJ, 980, 138, doi: [10.3847/1538-4357/ad9b2c](https://doi.org/10.3847/1538-4357/ad9b2c)
- Hartley, A. I., Nelson, E. J., Suess, K. A., et al. 2023, MNRAS, 522, 3138, doi: [10.1093/mnras/stad1162](https://doi.org/10.1093/mnras/stad1162)
- Hashimoto, T., Inoue, A. K., Mawatari, K., et al. 2019, PASJ, 71, 71, doi: [10.1093/pasj/psz049](https://doi.org/10.1093/pasj/psz049)
- Hatsukade, B., Kohno, K., Yamaguchi, Y., et al. 2018, PASJ, 70, 105, doi: [10.1093/pasj/psy104](https://doi.org/10.1093/pasj/psy104)
- Helton, J. M., Sun, F., Woodrum, C., et al. 2024, ApJ, 974, 41, doi: [10.3847/1538-4357/ad6867](https://doi.org/10.3847/1538-4357/ad6867)
- Herard-Demanche, T., Bouwens, R. J., Oesch, P. A., et al. 2025, MNRAS, 537, 788, doi: [10.1093/mnras/staf030](https://doi.org/10.1093/mnras/staf030)
- Hill, R., Scott, D., McLeod, D. J., et al. 2024, MNRAS, 528, 5019, doi: [10.1093/mnras/stae346](https://doi.org/10.1093/mnras/stae346)
- Hodge, J. A., & da Cunha, E. 2020, Royal Society Open Science, 7, 200556, doi: [10.1098/rsos.200556](https://doi.org/10.1098/rsos.200556)
- Hodge, J. A., Swinbank, A. M., Simpson, J. M., et al. 2016, ApJ, 833, 103, doi: [10.3847/1538-4357/833/1/103](https://doi.org/10.3847/1538-4357/833/1/103)
- Hsiao, T. Y.-Y., Álvarez-Márquez, J., Coe, D., et al. 2024, ApJ, 973, 81, doi: [10.3847/1538-4357/ad6562](https://doi.org/10.3847/1538-4357/ad6562)
- Hughes, D. H., Serjeant, S., Dunlop, J., et al. 1998, Nature, 394, 241, doi: [10.1038/28328](https://doi.org/10.1038/28328)
- Hygate, A. P. S., Hodge, J. A., da Cunha, E., et al. 2023, MNRAS, 524, 1775, doi: [10.1093/mnras/stad1212](https://doi.org/10.1093/mnras/stad1212)
- Inami, H., Algera, H. S. B., Schouws, S., et al. 2022, MNRAS, 515, 3126, doi: [10.1093/mnras/stac1779](https://doi.org/10.1093/mnras/stac1779)
- Ji, Z., Williams, C. C., Rieke, G. H., et al. 2024a, arXiv e-prints, arXiv:2409.17233, doi: [10.48550/arXiv.2409.17233](https://doi.org/10.48550/arXiv.2409.17233)
- Ji, Z., Williams, C. C., Suess, K. A., et al. 2024b, arXiv e-prints, arXiv:2401.00934, doi: [10.48550/arXiv.2401.00934](https://doi.org/10.48550/arXiv.2401.00934)
- Kannan, R., Garaldi, E., Smith, A., et al. 2022, MNRAS, 511, 4005, doi: [10.1093/mnras/stab3710](https://doi.org/10.1093/mnras/stab3710)
- Kashino, D., Lilly, S. J., Matthee, J., et al. 2023, ApJ, 950, 66, doi: [10.3847/1538-4357/acc588](https://doi.org/10.3847/1538-4357/acc588)
- Kennicutt, R. C., & Evans, N. J. 2012, ARA&A, 50, 531, doi: [10.1146/annurev-astro-081811-125610](https://doi.org/10.1146/annurev-astro-081811-125610)
- Kokorev, V., Chávez Ortiz, Ó. A., Taylor, A. J., et al. 2025, arXiv e-prints, arXiv:2504.12504, doi: [10.48550/arXiv.2504.12504](https://doi.org/10.48550/arXiv.2504.12504)
- Laporte, N., Zitrin, A., Ellis, R. S., et al. 2021, MNRAS, 505, 4838, doi: [10.1093/mnras/stab191](https://doi.org/10.1093/mnras/stab191)
- Leśniewska, A., & Michałowski, M. J. 2019, A&A, 624, L13, doi: [10.1051/0004-6361/201935149](https://doi.org/10.1051/0004-6361/201935149)
- Li, J., Venemans, B. P., Walter, F., et al. 2022, ApJ, 930, 27, doi: [10.3847/1538-4357/ac61d7](https://doi.org/10.3847/1538-4357/ac61d7)
- Li, Q., Conselice, C. J., Sarron, F., et al. 2025, MNRAS, 539, 1796, doi: [10.1093/mnras/staf543](https://doi.org/10.1093/mnras/staf543)
- Lim, C.-F., Wang, W.-H., Smail, I., et al. 2020, ApJ, 889, 80, doi: [10.3847/1538-4357/ab607f](https://doi.org/10.3847/1538-4357/ab607f)
- Lin, X., Fan, X., Wang, F., et al. 2025, arXiv e-prints, arXiv:2504.08039, doi: [10.48550/arXiv.2504.08039](https://doi.org/10.48550/arXiv.2504.08039)
- Long, A. S., Casey, C. M., McKinney, J., et al. 2024a, arXiv e-prints, arXiv:2408.14546, doi: [10.48550/arXiv.2408.14546](https://doi.org/10.48550/arXiv.2408.14546)
- Long, A. S., Antwi-Danso, J., Lambrides, E. L., et al. 2024b, ApJ, 970, 68, doi: [10.3847/1538-4357/ad4cea](https://doi.org/10.3847/1538-4357/ad4cea)
- Lovell, C. C., Roper, W., Vijayan, A. P., et al. 2023, MNRAS, 525, 5520, doi: [10.1093/mnras/stad2550](https://doi.org/10.1093/mnras/stad2550)
- Lutz, D., Poglitsch, A., Altieri, B., et al. 2011, A&A, 532, A90, doi: [10.1051/0004-6361/201117107](https://doi.org/10.1051/0004-6361/201117107)
- Lyu, J., Rieke, G. H., & Alberts, S. 2016, ApJ, 816, 85, doi: [10.3847/0004-637X/816/2/85](https://doi.org/10.3847/0004-637X/816/2/85)
- Ma, Z., Sun, B., Cheng, C., et al. 2024, ApJ, 975, 87, doi: [10.3847/1538-4357/ad7b32](https://doi.org/10.3847/1538-4357/ad7b32)
- Madau, P., & Dickinson, M. 2014, ARA&A, 52, 415, doi: [10.1146/annurev-astro-081811-125615](https://doi.org/10.1146/annurev-astro-081811-125615)
- Mazzucchelli, C., Decarli, R., Farina, E. P., et al. 2019, ApJ, 881, 163, doi: [10.3847/1538-4357/ab2f75](https://doi.org/10.3847/1538-4357/ab2f75)
- McKinney, J., Casey, C. M., Long, A. S., et al. 2025, ApJ, 979, 229, doi: [10.3847/1538-4357/ada357](https://doi.org/10.3847/1538-4357/ada357)
- Murray, S. G., Power, C., & Robotham, A. S. G. 2013, Astronomy and Computing, 3, 23, doi: [10.1016/j.ascom.2013.11.001](https://doi.org/10.1016/j.ascom.2013.11.001)
- Naidu, R. P., Oesch, P. A., Brammer, G., et al. 2025, arXiv e-prints, arXiv:2505.11263. <https://arxiv.org/abs/2505.11263>
- Nelson, D., Springel, V., Pillepich, A., et al. 2019, Computational Astrophysics and Cosmology, 6, 2, doi: [10.1186/s40668-019-0028-x](https://doi.org/10.1186/s40668-019-0028-x)
- Nguyen, H. T., Schulz, B., Levenson, L., et al. 2010, A&A, 518, L5, doi: [10.1051/0004-6361/201014680](https://doi.org/10.1051/0004-6361/201014680)
- Noll, S., Burgarella, D., Giovannoli, E., et al. 2009, A&A, 507, 1793, doi: [10.1051/0004-6361/200912497](https://doi.org/10.1051/0004-6361/200912497)
- Oke, J. B., & Gunn, J. E. 1983, ApJ, 266, 713, doi: [10.1086/160817](https://doi.org/10.1086/160817)
- Oliver, S. J., Bock, J., Altieri, B., et al. 2012, MNRAS, 424, 1614, doi: [10.1111/j.1365-2966.2012.20912.x](https://doi.org/10.1111/j.1365-2966.2012.20912.x)

- Pensabene, A., Decarli, R., Bañados, E., et al. 2021, *A&A*, 652, A66, doi: [10.1051/0004-6361/202039696](https://doi.org/10.1051/0004-6361/202039696)
- Pérez-González, P. G., Rinaldi, P., Caputi, K. I., et al. 2024, *ApJL*, 969, L10, doi: [10.3847/2041-8213/ad517b](https://doi.org/10.3847/2041-8213/ad517b)
- Pillepich, A., Nelson, D., Hernquist, L., et al. 2018, *MNRAS*, 475, 648, doi: [10.1093/mnras/stx3112](https://doi.org/10.1093/mnras/stx3112)
- Pizzati, E., Hennawi, J. F., Schaye, J., et al. 2024, *MNRAS*, 534, 3155, doi: [10.1093/mnras/stae2307](https://doi.org/10.1093/mnras/stae2307)
- Popping, G., Somerville, R. S., & Galametz, M. 2017, *MNRAS*, 471, 3152, doi: [10.1093/mnras/stx1545](https://doi.org/10.1093/mnras/stx1545)
- Pudoka, M., Wang, F., Fan, X., et al. 2025, arXiv e-prints, arXiv:2505.07932, doi: [10.48550/arXiv.2505.07932](https://doi.org/10.48550/arXiv.2505.07932)
- Riechers, D. A., Bradford, C. M., Clements, D. L., et al. 2013, *Nature*, 496, 329, doi: [10.1038/nature12050](https://doi.org/10.1038/nature12050)
- Rieke, G. H., Alberts, S., Shivaee, I., et al. 2024, *ApJ*, 975, 83, doi: [10.3847/1538-4357/ad6cd2](https://doi.org/10.3847/1538-4357/ad6cd2)
- Rieke, G. H., Alonso-Herrero, A., Weiner, B. J., et al. 2009, *ApJ*, 692, 556, doi: [10.1088/0004-637X/692/1/556](https://doi.org/10.1088/0004-637X/692/1/556)
- Rieke, M. J., Kelly, D. M., Misselt, K., et al. 2023, *PASP*, 135, 028001, doi: [10.1088/1538-3873/acac53](https://doi.org/10.1088/1538-3873/acac53)
- Rinaldi, P., Pérez-González, P. G., Rieke, G. H., et al. 2025, arXiv e-prints, arXiv:2504.01852, doi: [10.48550/arXiv.2504.01852](https://doi.org/10.48550/arXiv.2504.01852)
- Robertson, B., Johnson, B. D., Tacchella, S., et al. 2024, *ApJ*, 970, 31, doi: [10.3847/1538-4357/ad463d](https://doi.org/10.3847/1538-4357/ad463d)
- Shen, Y., Zhuang, M.-Y., Li, J., et al. 2024, arXiv e-prints, arXiv:2408.12713, doi: [10.48550/arXiv.2408.12713](https://doi.org/10.48550/arXiv.2408.12713)
- Silva, L., Granato, G. L., Bressan, A., & Danese, L. 1998, *ApJ*, 509, 103, doi: [10.1086/306476](https://doi.org/10.1086/306476)
- Simpson, J. M., Smail, I., Swinbank, A. M., et al. 2015, *ApJ*, 807, 128, doi: [10.1088/0004-637X/807/2/128](https://doi.org/10.1088/0004-637X/807/2/128)
- Simpson, J. M., Smail, I., Swinbank, A. M., et al. 2019, *ApJ*, 880, 43, doi: [10.3847/1538-4357/ab23ff](https://doi.org/10.3847/1538-4357/ab23ff)
- Smail, I., Ivison, R. J., & Blain, A. W. 1997, *ApJL*, 490, L5, doi: [10.1086/311017](https://doi.org/10.1086/311017)
- Snyder, G. F., Lotz, J. M., Rodriguez-Gomez, V., et al. 2017, *MNRAS*, 468, 207, doi: [10.1093/mnras/stx487](https://doi.org/10.1093/mnras/stx487)
- Strandet, M. L., Weiss, A., De Breuck, C., et al. 2017, *ApJL*, 842, L15, doi: [10.3847/2041-8213/aa74b0](https://doi.org/10.3847/2041-8213/aa74b0)
- Sun, F., Egami, E., Fujimoto, S., et al. 2022, *ApJ*, 932, 77, doi: [10.3847/1538-4357/ac6e3f](https://doi.org/10.3847/1538-4357/ac6e3f)
- Sun, F., Helton, J. M., Egami, E., et al. 2024, *ApJ*, 961, 69, doi: [10.3847/1538-4357/ad07e3](https://doi.org/10.3847/1538-4357/ad07e3)
- Sun, F., Wang, F., Yang, J., et al. 2025a, *ApJ*, 980, 12, doi: [10.3847/1538-4357/ad9d0e](https://doi.org/10.3847/1538-4357/ad9d0e)
- Sun, F., Fudamoto, Y., Lin, X., et al. 2025b, arXiv e-prints, arXiv:2503.15587, doi: [10.48550/arXiv.2503.15587](https://doi.org/10.48550/arXiv.2503.15587)
- Tamura, Y., Mawatari, K., Hashimoto, T., et al. 2019, *ApJ*, 874, 27, doi: [10.3847/1538-4357/ab0374](https://doi.org/10.3847/1538-4357/ab0374)
- Toft, S., Smolčić, V., Magnelli, B., et al. 2014, *ApJ*, 782, 68, doi: [10.1088/0004-637X/782/2/68](https://doi.org/10.1088/0004-637X/782/2/68)
- Turner, C., Tacchella, S., D'Eugenio, F., et al. 2025, *MNRAS*, 537, 1826, doi: [10.1093/mnras/staf128](https://doi.org/10.1093/mnras/staf128)
- Valentino, F., Brammer, G., Gould, K. M. L., et al. 2023, *ApJ*, 947, 20, doi: [10.3847/1538-4357/acbefa](https://doi.org/10.3847/1538-4357/acbefa)
- van Leeuwen, I. F., Bouwens, R. J., van der Werf, P. P., et al. 2024, *MNRAS*, 534, 2062, doi: [10.1093/mnras/stae2171](https://doi.org/10.1093/mnras/stae2171)
- Venemans, B. P., Neeleman, M., Walter, F., et al. 2019, *ApJL*, 874, L30, doi: [10.3847/2041-8213/ab11cc](https://doi.org/10.3847/2041-8213/ab11cc)
- Venemans, B. P., Walter, F., Neeleman, M., et al. 2020, *ApJ*, 904, 130, doi: [10.3847/1538-4357/abc563](https://doi.org/10.3847/1538-4357/abc563)
- Vieira, J. D., Crawford, T. M., Switzer, E. R., et al. 2010, *ApJ*, 719, 763, doi: [10.1088/0004-637X/719/1/763](https://doi.org/10.1088/0004-637X/719/1/763)
- Walter, F., Decarli, R., Carilli, C., et al. 2012, *Nature*, 486, 233, doi: [10.1038/nature11073](https://doi.org/10.1038/nature11073)
- Wang, F., Yang, J., Fan, X., et al. 2019, *ApJ*, 884, 30, doi: [10.3847/1538-4357/ab2be5](https://doi.org/10.3847/1538-4357/ab2be5)
- Wang, F., Fan, X., Yang, J., et al. 2021, *ApJ*, 908, 53, doi: [10.3847/1538-4357/abcc5e](https://doi.org/10.3847/1538-4357/abcc5e)
- Wang, F., Yang, J., Hennawi, J. F., et al. 2023, *ApJL*, 951, L4, doi: [10.3847/2041-8213/accd6f](https://doi.org/10.3847/2041-8213/accd6f)
- Wang, F., Yang, J., Hennawi, J. F., et al. in prep.,
- Wang, T., Schreiber, C., Elbaz, D., et al. 2019, *Nature*, 572, 211, doi: [10.1038/s41586-019-1452-4](https://doi.org/10.1038/s41586-019-1452-4)
- Watson, D., Christensen, L., Knudsen, K. K., et al. 2015, *Nature*, 519, 327, doi: [10.1038/nature14164](https://doi.org/10.1038/nature14164)
- Whitler, L., Stark, D. P., Topping, M. W., et al. 2025, arXiv e-prints, arXiv:2501.00984, doi: [10.48550/arXiv.2501.00984](https://doi.org/10.48550/arXiv.2501.00984)
- Williams, C. C., Alberts, S., Ji, Z., et al. 2024, *ApJ*, 968, 34, doi: [10.3847/1538-4357/ad3f17](https://doi.org/10.3847/1538-4357/ad3f17)
- Yamaguchi, Y., Kohno, K., Hatsukade, B., et al. 2019, *ApJ*, 878, 73, doi: [10.3847/1538-4357/ab0d22](https://doi.org/10.3847/1538-4357/ab0d22)
- Yang, J., Wang, F., Fan, X., et al. 2023, *ApJL*, 951, L5, doi: [10.3847/2041-8213/acc9c8](https://doi.org/10.3847/2041-8213/acc9c8)
- Yang, J., Wang, F., Hennawi, J. F., et al. in prep.,
- Zavala, J. A., Montaña, A., Hughes, D. H., et al. 2018, *Nature Astronomy*, 2, 56, doi: [10.1038/s41550-017-0297-8](https://doi.org/10.1038/s41550-017-0297-8)
- Zavala, J. A., Castellano, M., Akins, H. B., et al. 2025, *Nature Astronomy*, 9, 155, doi: [10.1038/s41550-024-02397-3](https://doi.org/10.1038/s41550-024-02397-3)
- Ziparo, F., Ferrara, A., Sommovigo, L., & Kohandel, M. 2023, *MNRAS*, 520, 2445, doi: [10.1093/mnras/stad125](https://doi.org/10.1093/mnras/stad125)
- Zitrin, A., Labbé, I., Belli, S., et al. 2015, *ApJL*, 810, L12, doi: [10.1088/2041-8205/810/1/L12](https://doi.org/10.1088/2041-8205/810/1/L12)